HYBRID DIVERSITY COMBINED OFDM FOR OPTICAL WIRELESS COMMUNICATION

By

Rumana Binte Faruque

MASTER OF SCIENCE IN

INFORMATION AND COMMUNICATION TECHNOLOGY

Institute of Information and Communication Technology

BANGLADESH UNIVERSITY OF ENGINEERING AND TECHNOLOGY

August 2017

The thesis titled **"HYBRID DIVERSITY COMBINED OFDM FOR OPTICAL WIRELESS COMMUNICATION"** Submitted by Rumana Binte Faruque, Roll No: 1014312029, Session: October 2014, has been accepted as satisfactory in partial fulfillment of the requirement for the degree of Master of Science in Information and Communication Technology on 12 August 2017.

BOARD OF EXAMINERS

1. _____

Dr. Md. Rubaiyat Hossain Mondal — Chairman
Associate Professor
Institute of Information and Communication Technology — (Supervisor)
BUET, Dhaka-1205

2. _____

Dr. Hossen Asiful Mustafa
Assistant Professor
Institute of Information and Communication Technology — Member
BUET, Dhaka-1205

3. _____

Dr. Md. Saiful Islam
Director — Member
Institute of Information and Communication Technology — (Ex officio)
BUET, Dhaka-1205

4. _____

Dr. Mohammad Abdul Matin
Professor — Member
Department of Electrical and Electronic Engineering — (External)
Northern University, Banani, Dhaka.

CANDIDATE'S DECLARATION

It is hereby declared that this thesis or any part of it has not been submitted elsewhere for the award of any degree or diploma.

Signature of the Candidate

_____

Rumana Binte Faruque

DEDICATED TO MY PARENTS

TABLE OF CONTENTS

LIST OF FIGURES

LIST OF ABBREVIATIONS

RF	Radio Frequency
OWC	Optical Wireless Communication
IR	Infrared
UV	Ultraviolet
LED	Light Emitting Diode
VLC	Visible Light Communication
SNR	Signal to Noise Ratio
MIMO	Multiple Input Multiple Output
OFDM	Orthogonal Frequency Division Multiplexing
DCO-OFDM	DC-biased optical OFDM
ACO-OFDM	Asymmetrically clipped optical OFDM
ADO-OFDM	Asymmetrically clipped DC-biased optical OFDM
DACO-OFDM	Diversity combined asymmetrically clipped ACO-OFDM
IM/DD	Intensity Modulation Direct Detection
ISI	Inter Symbol Interference
QAM	Quadrature Amplitude Modulation
CP	Cyclic Prefix
BER	Bit Error Rate
IFFT	Inverse Fast Fourier Transform

FFT	Fast Fourier Transform
LIFI	Light Fidelity
WIFI	Wireless Fidelity

LIST OF SYMBOLS

$E\{\bullet\}$	Expectation Operator
μ	Proportionality constant
$\sum$	Summation
σ	Standard deviation
*	Complex conjugate operator

ACKNOWLEDGEMENT

First of all, I would like to thank the Almighty for giving me the ability to complete this thesis work.

I would like to express my sincere gratitude to my supervisor, Dr. Md. Rubaiyat Hossain Mondal, Associate Professor of IICT, BUET. This thesis would not have been completed without his support and guidance. I would like to express my sincere thanks and gratefulness for his instructions, continuous encouragement, valuable discussions and careful scrutinization during the period of this research. I have been able to achieve a clear concept of optical wireless communication from him throughout the whole period, which I have utilized to develop my abilities to work innovatively. His constant encouragement gave me the confidence to carry out my work. It's a life-long achievement which will enable me to go a long way in becoming an independent researcher in the days ahead.

I would also like to thank all the teachers and staffs of IICT, BUET for their cordial help and assistance during my study period. Finally, I would like to thank my parents and family. Without their unconditional support, I would not have made it possible.

ABSTRACT

Optical Wireless Communication (OWC) in the visible spectrum provides the opportunity of high speed data transmission along with room illumination. In order to encode data for OWC, different variants of Orthogonal Frequency Division Multiplexing (OFDM) modulation are developed in the literature. Some of the most prominent ones are the direct current biased optical OFDM (DCO-OFDM), the asymmetrically clipped optical OFDM (ACO-OFDM), asymmetrically clipped DC biased optical OFDM (ADO-OFDM) and diversity-combined ACO-OFDM (DACO-OFDM). This thesis combines the aspects of DACO-OFDM and DCO-OFDM to develop a new modulation form termed as Hybrid Diversity Combined OFDM (HDC-OFDM) which has the benefits of power efficiency of DACO-OFDM and illumination capacity of DCO-OFDM. In HDC-OFDM transmitter, the lower subcarriers are modulated with DACO-OFDM, and the higher subcarriers with DCO-OFDM. When the DACO-OFDM and the DCO-OFDM signals are added, they impact one another. In order to remove the impact of DCO-OFDM clipping noise on DACO-OFDM component, a high DC bias is applied on DCO-OFDM which results in less clipping noise. On the other hand to reduce the effect of DACO-OFDM clipping noise on DCO-OFDM element, the DACO-OFDM clipping noise is estimated at the receiver and then deducted from the received signal of DCO-OFDM. In order to obtain the optimum bit error rate performance of HDC-OFDM, the percentage of subcarriers and the ratio of power levels for DACO-OFDM and for DCO-OFDM components are varied. Simulation results show that the BER performance of HDC-OFDM is the best when the portion of DACO-OFDM and DCO-OFDM elements are the same. Since the HDC-OFDM has a DCO-OFDM component, the dimming facility is easily achieved in HDC-OFDM by only increasing or decreasing the DC bias level without using any other additional modules or methods. Simulation results demonstrate that a dimming as low as 10% is also possible in HDC-OFDM at a 20 dB optical power degradation with respect to full brightness conditions. Simulation results also show that for a given data rate, the BER performance of HDC-OFDM is 5 dB better than DCO-OFDM, 1 dB better than ACO-OFDM, but only 1.5 dB inferior to DACO-OFDM. Therefore, the proposed HDC-OFDM has slightly less power efficiency than DACO-OFDM but achieves the simple dimming capability of DCO-OFDM.

CHAPTER 1

1 INTRODUCTION

1.1 Overview

The demand for reliable and high-speed wireless multimedia services is growing at a rapid pace. The use of laptops, smart phones, tablet computers, personal digital assistants (PDAs) and other portable terminals has become part of our day-to-day lives. At present, most wireless devices are based on radio frequency (RF) communication [1-3]. However, with the increase in bandwidth-intensive applications, the RF spectrum is becoming more and more congested. RF communication is also experiencing issues like spectrum licensing, security, electromagnetic interference etc. As a result, optical wireless communication (OWC) is being considered as a supplementary technique to RF communication. In a generalized OWC system, data are first modulated in the electrical domain and then converted to optical domain by an optical modulator. The transmitted optical signal is received by photodetectors. *Figure 1-1* shows the basic block diagram of a generalized OWC system where Laser diodes (LD) or LEDs are examples of optical modulators whereas positive-intrinsic-negative (PIN) photodiodes and avalanche photodiodes (APD) are some examples of photodetectors [4-10].

OWC has a number of advantages over RF. Firstly, a huge unregulated optical bandwidth is available for communication in the optical spectrum. OWC can be categorized into visible light communication (VLC) or infrared (IR) based on the frequency or wavelength of the optical signal. For both VLC and IR, the optical signal does not interfere with RF signal. In addition, optical signals are blocked by room walls and thus cannot be received by eavesdroppers. Optical signals can be made narrow and highly directional with the use of beam-shaping elements. Hence, information security is higher in OWC than RF wireless. OWC systems are usually of lower cost compared to RF systems [6-20]. However, the achievable data rates of OWC are restricted by the

modulation bandwidth of the optical modulators [4]. For instance, white LEDs offer only 20 MHz bandwidth. However, the data rate can be increased by the application of the multiple-input multiple-output (MIMO) technique, which is an advanced physical layer technology using a number of transmitting and receiving elements.

MIMO OWC using white LEDs can provide wireless internet service in addition to room lighting. This method is also known as light fidelity (LiFi). LiFi is often considered as an optical networked communication in the subset of VLC to offload the mobile data traffic which offers many advantages at indoor scenario. The lighting requirements for LiFi regulate the allowable transmitted optical power. For some other OWC links particularly infra-red based schemes, the concern of eye safety limits the transmitted optical power. Besides providing Internet connectivity, OWC can be used in secure data transmission, intelligence transportation system and communication in hospitals or aircrafts, etc. Indoor OWC are based on intensity modulation/direct detection (IM/DD) where the desired waveform is modulated onto the instantaneous power of the optical signal (i.e. the light intensity). Hence, the data-carrying transmitted signals have to be only unipolar or positive-valued [15-20].

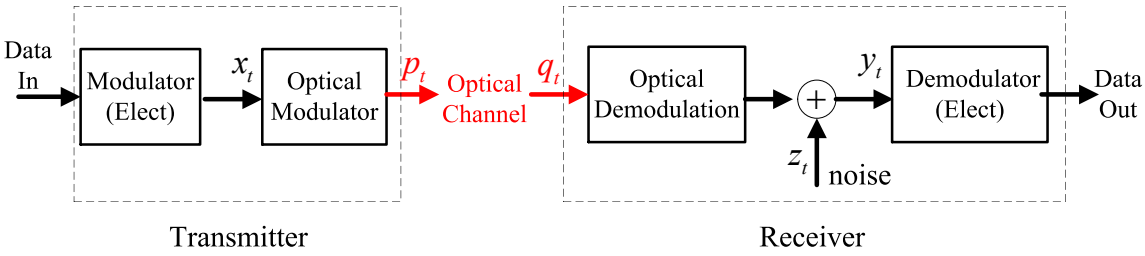

Figure 1-1: A block diagram of an OWC system

1.2 Motivation of the Thesis

Energy efficient design of communication systems including OWC is increasingly becoming important in the context of green environment. In this regard, the power efficiency of asymmetrically clipped optical OFDM (ACO-OFDM), diversity-combined ACO-OFDM (DACO-OFDM), direct current biased optical OFDM (DCO-OFDM) and

asymmetrically clipped DC biased optical OFDM (ADO-OFDM) [22] has been compared in a number of research papers. In [22, 55], it has been shown that ACO-OFDM is approximately 4.5 dB more optically power efficient than DCO-OFDM for a specific DC bias value. The required bias level for DCO-OFDM has been demonstrated for a 2-D spatial channel. The use of different bias levels is also shown for ADO-OFDM in [22]. With the selection of an optimum DC bias value, DCO-OFDM can have comparable performance as ACO-OFDM in terms of optical power. ADO-OFDM is shown to have slightly better BER performance than both ACO-OFDM and DCO-OFDM in some particular scenarios, but for many cases ADO-OFDM does not show comparable performance as ACO-OFDM and DCO-OFDM [22]. It is shown in [52] that theoretically, DACO-OFDM can have a gain of 3 dB over ACO-OFDM. Therefore, DACO-OFDM has the potential to be more power efficient than its counterparts. However, when room illumination is considered, DCO-OFDM is much more flexible than other OFDM formats. Therefore, there is a need to develop a modulation scheme which has the benefits of power efficiency and illumination capacity. In order to achieve both of these benefits simultaneously, this research focuses on combining the aspects of DACO-OFDM and DCO-OFDM for forming a new modulation scheme termed as Hybrid Diversity Combined OFDM (HDC-OFDM).

1.3 Objective of the Thesis

The objective of this work is to propose the idea of HDC-OFDM suitable for OWC and room illumination simultaneously. To fulfill the objective, the following analysis will be carried out:

1. Developing the concept of HDC-OFDM using the aspects of DACO-OFDM and DCO-OFDM.

2. Evaluating the BER performance of HDC-OFDM for the case of different factors including varying the subcarrier proportion and power proportion of DCO-OFDM in HDC-OFDM, constellation size and total number of subcarriers.

3. Comparing HDC-OFDM with DCO-OFDM, ACO-OFDM and DACO-OFDM in terms of BER performance and room illumination capacity.

1.4 Main Contributions of the Thesis

The main contributions of the thesis are as follows:

i) A framework for the proposed 'HDC-OFDM' modulation is developed combining the aspects of DCO-OFDM and DACO-OFDM. The merging of DCO-OFDM and DACO-OFDM is not straightforward. The DACO-OFDM is computed on low-index subcarriers while DCO-OFDM on high-index subcarriers. When these two signals are added, they impact one another. The clipping noise generated on DCO-OFDM signal impairs the performance of DACO-OFDM element. This is reduced by using a high DC bias on DCO-OFDM which results in less clipping noise. On the other hand, when DACO-OFDM signal is generated in the transmitter side, a clipping noise is formed affecting the DCO-OFDM signal. At the receiver side, the DACO-OFDM clipping noise is estimated and then deducted from the received signal of DCO-OFDM.

ii) The proportion of DACO-OFDM and DCO-OFDM elements in HDC-OFDM that results in the best BER performance is investigated in this thesis. It is shown in this work that the optimum BER results is achieved when half the subcarriers are modulated by DCO-OFDM and the other half by DACO-OFDM – where the power levels on these two signals are set equal.

1.5 Outline of the Thesis

The descriptions of the chapters to follow are provided below:

In **Chapter 2**, a detailed discussion of Optical Wireless System (OWC) with necessary block diagram of transmitter, receiver, channel condition and most importantly, room illumination with OWC will be presented to understand the basic concept of such a system. The important two branches of optical OFDM, namely DCO-OFDM and ACO-OFDM, will also be thoroughly presented. To understand Diversity-combined ACO-OFDM, it is required to understand the basic concepts of DCO-OFDM and ACO-OFDM

which will be discussed in this chapter. Furthermore, the detailed description of Diversity-combined ACO-OFDM will also be provided.

Chapter 3 will present the literature review of the previous research works related with diversity-combined optical ACO-OFDM. It will help to realize the increasing attention of such system for further research and the progress of technology in this field. The achievable data rates and different impairments that affect the system discussed in previous papers will also be presented here.

The performance of the proposed Hybrid Diversity Combined ACO-OFDM system will be evaluated in **Chapter 4**. Moreover, the performance will be compared in this chapter with existing optical OFDM schemes in terms of BER performance and illumination capacity.

A summary, conclusion and future direction of the thesis work will be presented in **Chapter 5**.

CHAPTER 2

2 OFDM for Optical Wireless Communication

2.1 Overview

The detailed description of the optical wireless system has been provided in this chapter with the detail design of the transmitter and receiver. OWC has been presented as a complementary solution to address the problems associated with the RF communication. Factors related with room illumination have also been stated as it is incorporated along with data communication. Different modulation schemes adopted for making the bipolar signal unipolar has also been delineated with the detailed description of transmitter, receiver and their corresponding statistics performance.

2.2 Optical Wireless Communication Complementing RF Communication

RF communication is the mostly availed communication facility as it facilitates quick and reliable deployment of a communication network. But, this technology only permits data rates up to several hundreds of megabits per second for RF WLANs and for point-to-point links [1-3]. Moreover, the problems of information security (eavesdropping), spectrum licensing as well as interference problems are significant issues in high speed data transfer using RF links. OWC has emerged to be a viable solution complementing RF communication while addressing most of the aforementioned problems. It allows the transmission of data rates up to several gigabits per second in point-to-point communication links. Indoor optical WLANs, device-to-device communication protocols (e.g. IrDA) and FSO are some of the potential application areas of OWC [7].

OWC systems have recently attracted much interest as VLC is being applied via white LEDs allowing transmission of information along with providing illumination. White LEDs have become extremely popular as lighting devices mainly because of increased energy efficiency compared to incandescent and fluorescent lamps. Data rates of hundreds of megabits per second can be achieved with white LEDs in indoor OWC systems [21-29].

2.3 Intensity Modulation/Direct Detection (IM/DD) in Optical Wireless System

Information is transmitted on the intensity or instantaneous power of the light in Intensity Modulation (IM) scheme and DD (Direct Detection) is the process where an electrical signal is produced at the receiver which is a replica of the intensity of the optical signal. A laser diode or an LED is used to modulate the transmitted signal in an IM/DD system given that laser and LED emissions should conform to the guidelines of international standard bodies such as the American National Standards Institute (ANSI) and the International Electrotechnical Commission (IEC). In the receiver side, a photodetector is used for performing DD in IM/DD systems because light is usually received in several electromagnetic modes. This overall process makes it difficult to construct an efficient down-converter at the receiver side for collecting appreciable power from a single mode. The two mostly used types of indoor IM/DD OWC systems are IR based indoor IM/DD OWC and visible light based indoor IM/DD OWC systems. Eye safety regulations must be conformed to while transmitting via IR (Infrared Ray) for it is invisible to the naked eye. High IR radiation can be highly dangerous to human eyes. On the contrary, human eye adjusts to light in the visible range, so white LEDs used in visible light based indoor IM/DD OWC systems are normally considered eye safe [25-35].

2.4 Advantages and Disadvantages of an Indoor IM/DD OWC system

Secure communication is one of the key features of an indoor IM/DD OWC system. Eavesdropping is impossible in this system for light does not have the ability to travel through opaque objects and hence optical signals are confined to the room where they

are operating in. Secondly, RF interference is not an issue as light in the different frequency bandwidth is being used to transmit information. In places of multiple personal or professional interests such as hospitals, airports and factories where many RF devices are employed already, indoor IM/DD OWC systems can operate in conjunction with RF systems without mutual interference. Thirdly, an LED at the transmitter, a photodiode at the receiver as direct detector along with baseband signal processing provide the ease of using simple circuitry. Fourthly, Capability of isolating subnets in a network helps in prevention of any signal crosstalk or connection between access points. Last but not the least, OWC system operating in one indoor room is separate from one operating in another room [28-34].

Several disadvantages are associated with an IM/DD optical wireless system such as the presence of ambient light. Indoor IM/DD systems operating using visible light are detrimentally affected by ambient light sources such as sunlight, light from fluorescent lamps and incandescent lamps, etc. This interference from so many sources makes it difficult to differentiate between the wanted signal and the interfering signal. Shot noise is also a limiting factor at the receiver side. Furthermore, mobility is restricted in this system due to the inability of light to penetrate opaque objects. Another disadvantage is the limited performance of an indoor IM/DD system in the absence of LOS due to the high path loss and signal degradation [22-26, 29-33].

2.5 Modulation Schemes in Indoor IM/DD OWC Systems

On-Off Keying (OOK) and Pulse Position Modulation (PPM) are two conventionally used modulation schemes in indoor IM/DD OWC systems. But recently, Orthogonal Frequency Division Multiplexing (OFDM) has drawn attention as a possible modulation scheme due to its high optical power efficiency and robustness to Inter-Symbol Interference [4, 21-22]. Several reasons lie behind the choice of IM/DD OWC systems as a modulation scheme and one of them is the increased optical power efficiency when large constellations are used. It also shows good resistance against the low frequency interference from sources such as fluorescent lights. It must be noted that zeroth frequency subcarrier is usually affected by such interference. At OFDM, this problem is

minimized by avoiding the zeroth subcarrier at the time of demodulation. It also gives the provision for adaptive modulation to be performed which is very important in an IM/DD OWC system due to the low pass characteristics of an indoor optical communication channel. The main theme of adaptive modulation is that smaller constellations supporting fewer bits can be used on high frequency subcarriers having poor channel quality; whereas larger constellations modulation schemes capable of transmitting more bits can be used on lower frequency subcarriers with good channel quality.

The instantaneous power of light is used for modulation in indoor IM/DD OWC systems. Hence, a conventional OFDM signal cannot be applied to a typical IM/DD system for the signal is bipolar and complex. This calls for the fact that the transmitted optical OFDM signal has to be both positive as well as real. The condition of Hermitian Symmetry has to be imposed on the subcarriers in order to make the output signal real.

2.6 Optical Wireless System

The design of the OWC transmitter, receiver and channel is described below for a better understanding of the whole system:

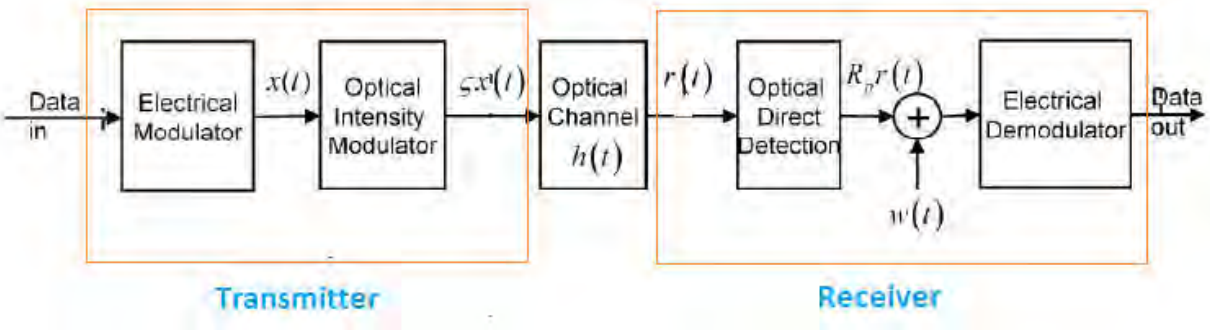

Figure 2-1 Block Diagram of an indoor OWC system

2.6.1 Transmitter

The total Optical Wireless System is described with the help of the block diagram of Figure 2-1. The transmitter is the first block of the Intensity Modulation Direct Detection

(IM/DD) optical wireless system (OWC) and electrical modulator is the first block of the transmitter. The main purpose of this block is to map the data to a modulation scheme such as Orthogonal Frequency Division Multiplexing (OFDM). $x(t)$ is the electrical signal at the output of the electrical modulator. It is sent to the optical intensity modulator where an optical signal with intensity, $\varepsilon x(t)$ is generated, where the coefficient ε is the electrical-to-optical conversion efficiency. It is assumed in this thesis that $\varepsilon = 1$ (for simplicity and without loss of generality).

Usually, the optical signal intensity is approximately proportional to the electrical current modulating the LED, $x(t)$. The main factors, while designing the block, are that the average optical power which is directly proportional to signal $x(t)$ and the average electrical power which is directly proportional to $x^2(t)$. The average optical power is denoted by $E\{x(t)\}$ and the average electrical power is defined as $E\{x^2(t)\}$.

The white LED is usually used as a modulator and they tend to show low pass characteristics. A phosphor-based white LED which has a modulation bandwidth of 2 MHz is a common type of white LED used largely in indoor wireless VLC system. But by detecting only the blue component of the LED emission, an increased modulation bandwidth upto 20 MHz is achievable.

In order to broadcast information to receiving devices such as laptops and mobile phones that operate within its range, white LEDs are usually used as transmitters in VLC systems. But, as LEDs are normally situated on the ceilings and not in laptops, employing white LEDs in the uplink in an indoor IM/DD OWC system is quite challenging. That is the main reason for using IR or RF beams for the uplink in these systems. Hence, for a terminal inside an optical hotspot similar to a wireless fidelity (Wi-Fi) hotspot, an optical link is used for the downlink and an RF link is used for uplink. On the contrary, in case of a terminal outside the range of optical hotspot, RF can be used for both the uplink and the downlink.

2.6.2 Optical Wireless Channel

Both an Line of Sight (LOS) component and multiple reflected paths can be present between the transmitter and the receiver in an optical wireless system. The direct path between the transmitter and the receiver is called the LOS component whereas signals bounced off the ceiling, walls and other obstacles before reaching the receiver are called reflected components. The availability of a strong LOS path paves the way to approximating an optical wireless channel as a flat channel because the LOS component shows the lowest attenuation and high data rate communication can take place.

On the contrary, where a weak or no LOS path is present, the channel can be approximated as a baseband low-pass filter. The signal which has a very narrow and near-zero frequency range, i.e., a spectral magnitude that is nonzero only for frequencies in the vicinity of the origin (termed $f = 0$) and negligible elsewhere; is called a baseband signal. The bandwidth of an indoor OWC channel is dependent on the size of the room meaning that a large room results in low channel bandwidth.

2.6.3 Receiver

The optical signal is firstly converted from the optical to electrical domain by using a photodiode at the receiver side. Photodiode is a reverse biased diode where free electron-hole pairs are generated after the incidence of sufficient optical energy upon it. $r(t)$ is the received optical signal, $R_p r(t)$ is the output signal after the direct detection process, where the coefficient R_p is the photodiode responsivity.

The shot noise at the detector affects the optical wireless systems. The random electron-hole pairs generated in the p-n junction of a photodiode due to incident photons are mainly responsible for shot noise. It is modeled as $n(t)$, an AWGN, added in the electrical domain. An optical filter which filters the ambient light reaching a photodiode while only passing the optical signal $x(t)$ can reduce the shot noise to a great extent.

Narrowband optical filter is sufficient for lasers due to narrow optical bandwidth; while on the contrary, LEDs require optical filters with large bandwidths as they have large optical bandwidth. The preamplifier noise which is independent and Gaussian is the dominant noise source when no background light is present. An electrical current proportional to the intensity of light is generated by the photodiode. The diameter of a photodiode used in an indoor IM/DD OWC is many times larger than the wavelength of the transmitted optical signal. This is the reason of prevalence of path differences when optical signals arrive at different points of the photodiode. Moreover, this phenomenon results in the low pass characteristics of the photodiode.

Two types of photodiodes are mainly used in indoor Intensity Modulation/Direct Detection systems, namely positive-intrinsic-negative (PIN) photodiode and avalanche photodiode (APD). APDs are temperature dependent and generate high photocurrent compared to PIN diodes. This phenomenon makes them very expensive compared to other photodiodes. But its performance deteriorates in the presence of ambient light for it does not increase the SNR as required. This is due to the internal gain of APD increasing the spectral density of shot noise by a factor greater than the signal gain. Finally, the resultant electrical signal at the output of the DD module is delivered to the data detection module for signal processing and further detection.

2.7 Room Illumination with OWC

For the case of Optical data transmission, illuminating the room as well as dimming the LEDs has always been a crucial problem to address because the lighting requirement may be different depending on time, location, weather and most importantly, comfort to the human eye. Eye safety regulation is another concern in this case. From logical point of view, the brightness increases with the current but there is a limit of tolerance to human eyes for the brightness of the LEDs. Lighting control is a special feature incorporated in the modern sophisticated apartments and most importantly corporate offices as lighting controls can increase the value of buildings by making them productive, comfortable and energy efficient; which is a direct product of dimming functionality. Dimming is highly application specific for instance, settings such as office

rooms, conference rooms or examination rooms can require light levels as low as 1% of maximum illumination for aesthetic and comfort purposes.

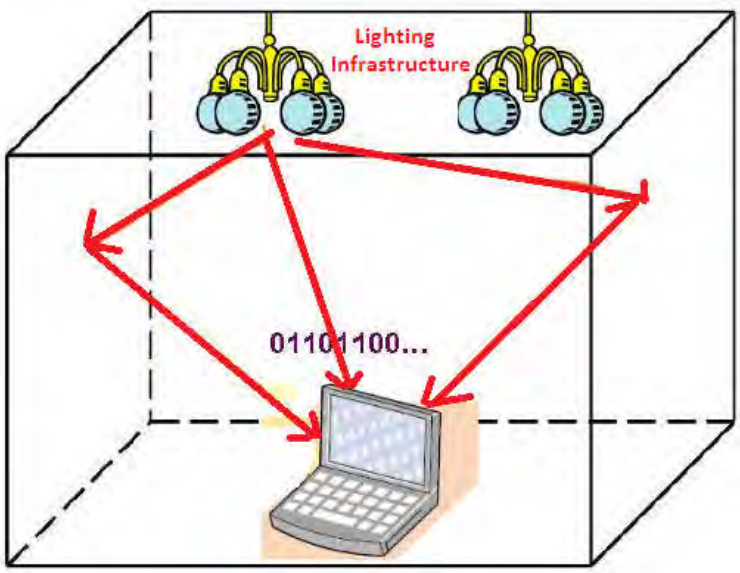

Figure 2-2 Illustration of data communication and room illumination in an indoor OWC system

Analog dimming, also known as amplitude modulation (AM) or Continuous Current Reduction (CCR), and digital dimming are the most noteworthy techniques adopted for this purpose. Pulse Width Modulation (PWM) is the simplest example of digital dimming modulation technique. In the PWM scheme, the duty cycle of the forward current is changed while brightness control is achieved by decreasing the forward current in CCR. In PWM, the time period of the signal is kept fixed whereas the duty cycle, D is varied proportionally to the required dimming percentage. In CCR, the luminous intensity is reduced proportionally to the current and a brightness level of 10% of maximum is achievable. Reducing current is the most cost-effective solution to realize dimming in LEDs. For industry purposes PWM is mostly recommended for it provides a large dimming range where linear relationship is maintained between the light output and duty cycle. LEDs also show low chromaticity shift in this process. The best color stability is offered by the CCR technique due to the counteracting influences of drive current and junction temperature variations whereas an LED suffers from constantly non-eliminable chromaticity changes while PWM is used.

In the case of dimming, transmitted optical power refers to the average optical power emitted by an LED chip, sum of the signal power (including the non-linear distortion effects) and DC-bias point induced optical power. At 90mW optical power, the lower limit is defined for illumination which is around 10% whereas a full brightness is considered at 0.4 W transmitted optical power. It can be noted that 35% brightness/dimming corresponds to the optical power of the recommended bias point which is found from the datasheet (350mA/180mW). From the curves and equations in [62], it has been shown that for 10% brightness, the illumination is below 320 lx, exactly appropriate in case of insufficient daylight while LED is used for the supplementary illumination. On the contrary, the illumination is above 550 lx for 35% brightness which guarantees a well-lit office.

In the case of ACO-OFDM, spectral efficiency is a major concern because only half of the transmitted subcarriers are used to carry the data symbols. Hence, a dimming scheme which is spectrum-efficient is of dire necessity. In terms of spectral efficiency and bit-error performance, PWM based dimming scheme offers better performance over Amplitude Modulation (AM) based scheme. In AM, the ACO-OFDM signal is superimposed on a fixed bias level leading to reduced LED dynamic range for transmission and the ACO-OFDM signal power also has to be optimized for each bias level and furthermore, the performance is directly related to the dimming set-point.

On the contrary, in PWM, ACO-OFDM clipping is avoided for a large amplitude-range of OFDM samples as the full dynamic range is being utilized. Avoidance of clipping helps to retain the shape of the transmitted signal waveshape and preserving the OFDM signal shape corresponds to less induced clipping noise allowing for higher order constellations providing better spectral efficiency or the establishment of more robust links (better BER).

2.8 Performance Metric for OWC

In communication theory, achieving reliable high data rate transmission with limited transmission power is important. In a practical system such as room illumination and

data communication via LiFi, there is a limitation on the average optical power that can be transmitted. Moreover, battery operated devices need high electrical power efficiency. Therefore, like most of the previous research papers, this thesis considers both average electrical and optical power as the limiting factor.

The power efficiency metric is different for average optical power and average electrical power limited channels. For the transmitted electrical signal s_l, the average optical power depends on $E\{s_l\}$ and the average electrical power depends on $E\{s_l^2\}$ where $E\{\bullet\}$ is the expectation operator. Hence, the conversion between optical power and electrical power depends on the statistics of s_l. For a fixed $E\{s_l\}$, a modulation scheme with high electrical-to-optical power ratio $E\{s_l^2\}/E\{s_l\}$ gives better BER.

Two performance metrics can be used to compare different modulation schemes. These are $E_{b(elec)}/N_0$, the received electrical energy per bit to single-sided noise spectral density, and $E_{b(opt)}/N_0$, the received optical energy per bit to single-sided noise spectral density. Unlike $E_{b(elec)}/N_0$, $E_{b(opt)}/N_0$ takes into account the optical-to-electrical conversion efficiency of the system, and thus, it is more useful as a performance metric. In this thesis, both $E_{b(elec)}/N_0$ and $E_{b(opt)}/N_0$ are considered as metrics and these two can be expressed in general as E_b/N_0.

2.9 Different OFDM Forms Used in OWC

For the better understanding of an optical OFDM system, a block diagram is in *Figure 2-3* delineating the whole process:

At the transmitter, the data is mapped onto 4-QAM, 16-QAM or the required modulation scheme, then converted from serial to parallel and given as the input to the IFFT block. Afterwards, the bipolar signal is made unipolar and this system differs from system to system. Next, the unipolar signal is converted from parallel to serial and Cyclic Prefix is

added, converted from Digital to Analog and then low pass filtered. The next step is to convert it into optical domain and pass it through the optical channel.

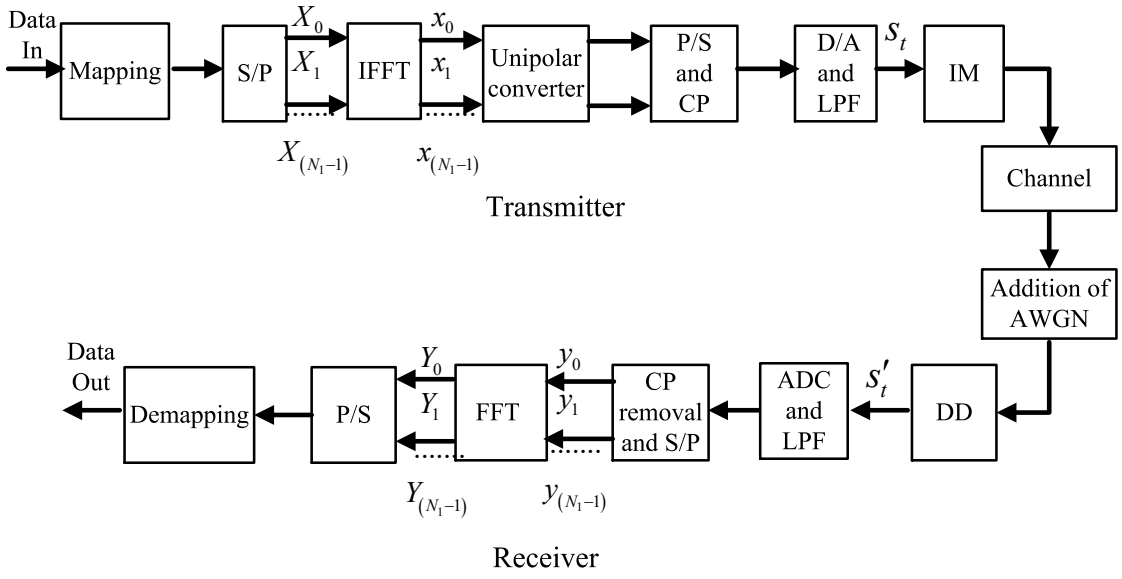

Figure 2-3 Block diagram of a generalized optical OFDM system

At the receiver side, the data is converted from analog to digital and low pass filtered after adding AWGN noise to it. Afterwards, cyclic prefix is removed and the data is given as an input to the FFT block after serial to parallel conversion. At last, the data is again converted from parallel to serial and demodulated at the receiver. In a nutshell, this is the total process which is followed in an OFDM system.

Different approaches have been adopted for making the real signal positive such as: DCO-OFDM [46, 54, 55], ACO-OFDM [46, 54, 55], ADO-OFDM and DACO-OFDM [51,52, 58]. Each of these OFDM forms has its own characteristics and is suitable for different application scenarios. These are the commonly used IM/DD modulation schemes being applied in Optical Wireless Systems now-a-days. The detailed description, performance evaluation as well as practical limitations of DCO-OFDM system, ACO-OFDM system and Diversity-combined ACO-OFDM system are delineated below:

2.9.1 DCO-OFDM

DCO-OFDM is an improvised OFDM system where a DC bias is added to the bipolar OFDM signal and the remaining negative peaks are clipped. Carruthers and Kahn were the first to propose this system. Clipping noise is introduced due to the negative clipping. Both odd and even subcarriers are incorporated for carrying data symbols and all of them are affected by the clipping noise.

The additional features or modules added in the transmitter of a DCO-OFDM system are the Hermitian symmetry module and the other one performs addition of a DC bias to the signal to be transmitted and clips any remaining negative peaks. The DCO OFDM receiver is just the same as the conventional OFDM receiver.

OFDM signals typically possess a very high peak-to-average power ratio (PAPR); so a very high bias is needed to remove all the negative peaks. But, it is very power consuming and decreases the power efficiency. Henceforth, a moderate bias is normally chosen and the remaining negative peaks are clipped. The biased signal is then input to an LED or laser which performs intensity modulation on an optical career. This resulting signal is then transmitted across an indoor optical wireless channel. Shot noise which is added in the electrical domain and affects the signal is modeled as AWGN.

At the receiver, the received signal is first converted from an optical signal to an electrical signal using a photodiode. The remaining process is just the same as the conventional OFDM receiver. In DCO-OFDM, all the subcarriers are demodulated as they all carry data symbols.

2.9.1.1 DCO-OFDM Transmitter and Receiver

In the transmitter, the input complex signal into the IFFT is given by $X = \left[X_0, X_1, X_2, \ldots..X_{N-1}\right]$. The X vector is constrained to have Hermitian symmetry and the two components X_0 and $X_{N/2}$ are set to zero, i.e. $X_0 = X_{N/2} = 0$,

$$X_m = X^*_{N-m} \quad \text{for} \quad 0 < m < N/2 \tag{2.1}$$

The Hermitian symmetry is needed to ensure that all the outputs at the output of the IFFT, x is real. The signal is then converted from parallel to serial (P/S), a Cyclic Prefix (CP) is appended, Digital to Analog converted and low pass filtered.

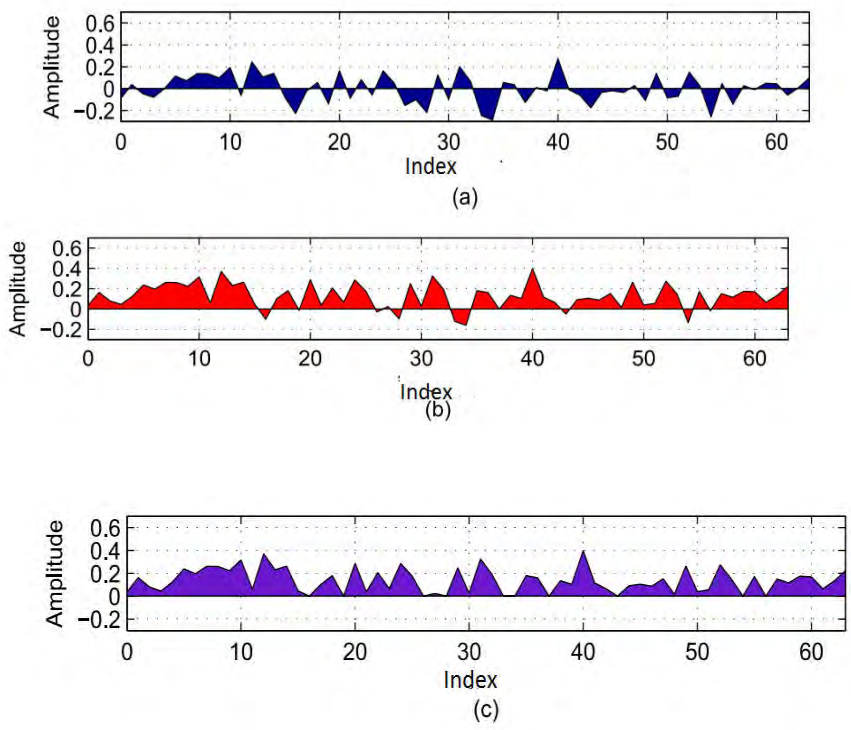

Figure 2-4: (a) signal $x(t)$ (b) signal $x(t)$ after addition of $K_{DC} = 3dB$ (c) signal $x_{DCO(t)}$ [22]

In Figure 2-4, the bipolar signal $x(t)$ is shown. Figure 2.1 presents signal $x(t)$ when a DC bias of $K_{DC} = 3\ dB$ is added to the same. After the addition of DC bias, only a few negative peaks are present. In Figure 2-4, signal $x_{DCO(t)}$ is shown where the negative peaks are clipped at zero. The DC bias level, K_{DC} can be defined relative to the standard deviation of $x(t)$,

$$K_{DC} = \mu \sqrt{E\left\{x(t)^2\right\}} \tag{2.2}$$

Where, μ is a proportionality constant and K_{DC} is the bias defined by this: $10log_{10}\left(\mu^2+1\right)$ dB.

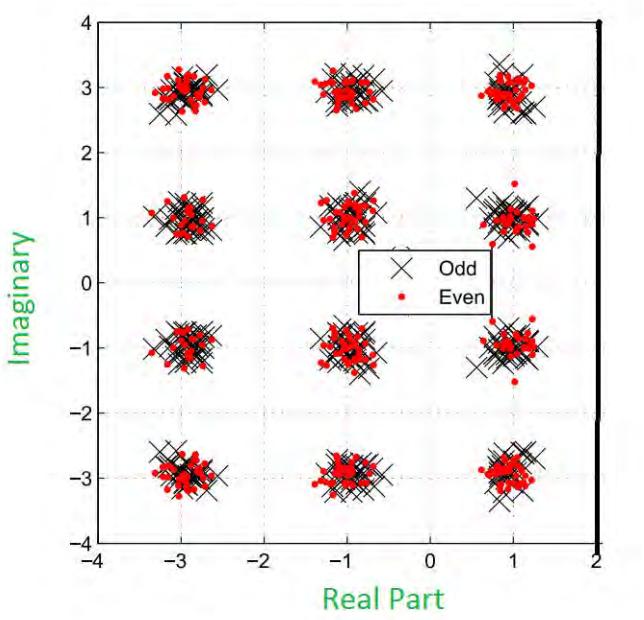

Figure 2-5 The Constellation of a 16-QAM DCO-OFDM signal without the effect of channel noise [22]

In *Figure 2-5*, the constellation diagram of $x_{DCO(t)}$ is shown for the system in the absence of channel noise. Constellation diagram is plotted for 16-QAM OFDM when the DC bias level is 7 dB. In the figure, the odd subcarriers and even subcarriers are represented by black crosses and red dots respectively (The constellation points are shown after the DC bias is removed). Noise like interference pattern can be seen in both odd and even subcarriers due to the DCO OFDM clipping noise.

2.9.1.2 Statistics and Performance of a DCO-OFDM System

In case of a large number of subcarriers, the unclipped continuous time domain signal, $x(t)$, can be modeled as a Gaussian random variable with zero mean and a

variance of $\sigma_D^2 = E\left\{x_k^{\,2}\right\}$ using the central limit theorem, where σ_D is the standard deviation of the unclipped signal. The optical power of DCO-OFDM, $P_{opt,DCO}$ can be easily derived using the PDF (Power Density Function) of DCO-OFDM. Hence,

$$\begin{aligned} P_{opt,DCO} &= E\{\mathrm{x}_{DCO}(\mathrm{t})\} = \int_0^\infty \psi f_{xDCO(\mathrm{t})}(\psi)\,\mathrm{d}\psi \\ &= \frac{\sigma_D}{2\pi}\, e\left(\frac{-K_{DC}^{\,2}}{2\sigma_D^{\,2}}\right) + B_{DC}\left(1 - Q\left(\frac{K_{DC}}{\sigma_D}\right)\right) \end{aligned} \tag{2.3}$$

$$\text{Where, } Q(\varepsilon) = \frac{1}{\sqrt{2\pi}} \int_\varepsilon^\infty e\left(-\frac{\beta^2}{2}\right) d\beta \tag{2.4}$$

Similarly, the electrical power of DCO-OFDM, $P_{opt,DCO}$ is :

$$\begin{aligned} P_{elec,DCO} &= E\{\mathrm{x}_{DCO(t)}^2\} = \int_0^\infty \psi^{\,2} f_{xDCO(\mathrm{t})}(\psi)\,\mathrm{d}\psi \\ &= (\sigma_D^2 + \mathrm{K}_{DC}^2)(1 - \mathrm{Q}\left(\frac{K_{DC}}{\sigma_D}\right)) + \frac{\sigma_D K_{DC}}{\sqrt{2\pi}}\, e\left(\frac{-\mathrm{K}_{DC}^2}{2\sigma_D^2}\right) \end{aligned} \tag{2.5}$$

The $E_{b(elec)} / N_0$ for DCO-OFDM is denoted by $E\left\{x_{DCO(t)}^2\right\} / b_{DCO} N_0$ and the $E_{b(opt)} / N_0$ for DCO-OFDM is denoted by $E\left\{x_{DCO(t)}\right\} / b_{DCO} N_0$, where b_{DCO} is the bit rate of DCO-OFDM.

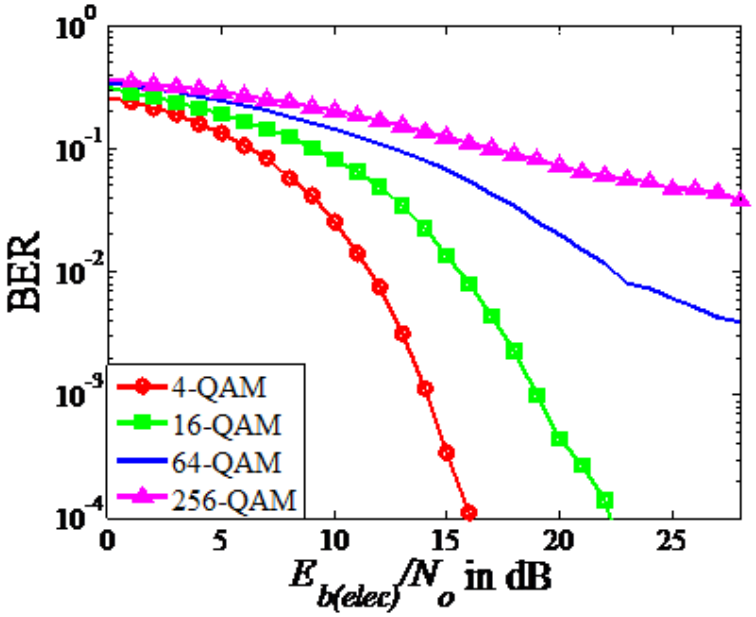

Figure 2-6 BER against $E_{b(elec)} / N_0$ curves of DCO-OFDM for 4-QAM, 16-QAM, 64-QAM and 256-QAM with a DC bias of 7 dB

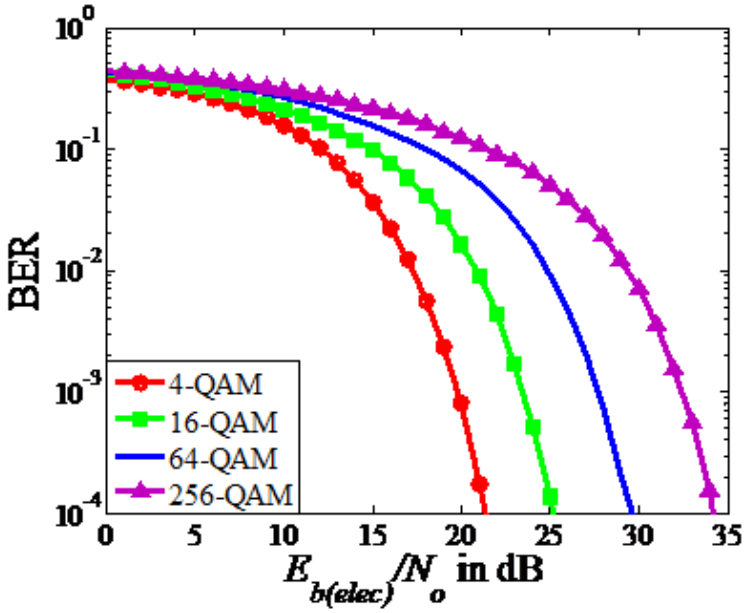

Figure 2-7 BER against $E_{b(elec)} / N_0$ curves of DCO-OFDM for 4-QAM, 16-QAM, 64-QAM and 256-QAM with a DC bias of 13 dB

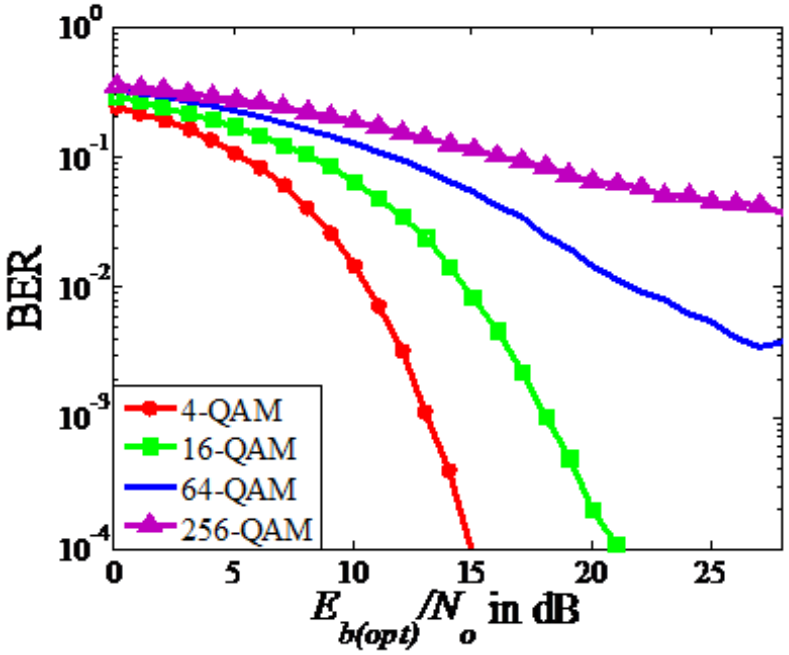

Figure 2-8 BER against $E_{b(opt)} / N_0$ curves of DCO-OFDM for 4-QAM, 16-QAM, 64-QAM and 256-QAM with a DC bias of 7 dB

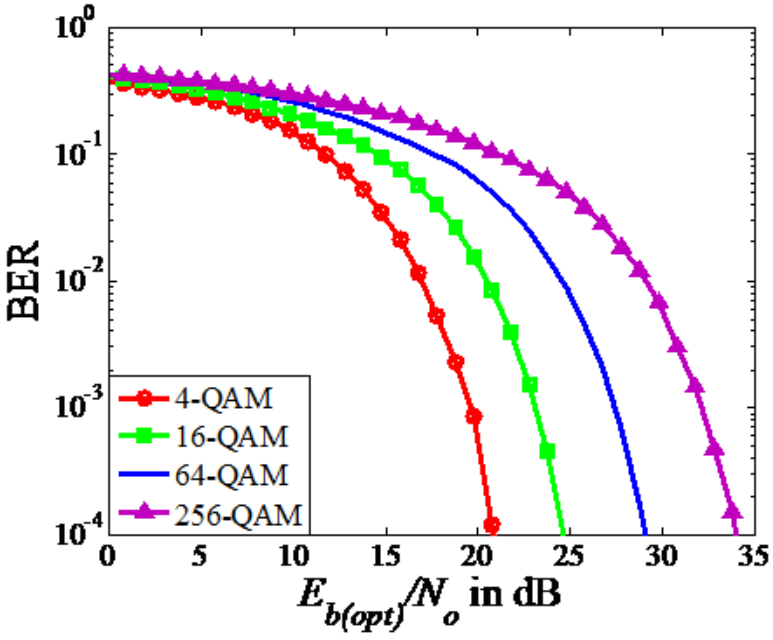

Figure 2-9 BER against $E_{b(opt)} / N_0$ curves of DCO-OFDM for 4-QAM, 16-QAM, 64-QAM and 256-QAM with a DC bias of 13 dB

In Figure 2-6, the BER against $E_{b(elec)} / N_0$ of DCO-OFDM for 4-QAM, 16-QAM, 64-QAM and 256-QAM are shown. The DC bias level on each of them is 7 dB. Large constellations such as 64-QAM and 256-QAM require high receiver SNRs. But when a larger bias such as 13 dB is used, the bit errors due to the DCO-OFDM clipping, reduce and the required receiver SNR as well as $E_{b(elec)} / N_0$ increases more. In Figure 2-7 it has been demonstrated by plotting BER against $E_{b(elec)} / N_0$ curves for 64-QAM and 256-QAM DCO-OFDM, where the DC bias level is set to 13 dB. The required $E_{b(elec)} / N_0$ increases as the DC bias level is increased more and more. For example, 4-QAM with a DC bias level of 13 dB requires higher $E_{b(elec)} / N_0$ for a BER of 10^{-3} than 4-QAM with a DC bias level of 7 dB.

In *Figure 2-8* and *Figure 2-9*, $E_{b(opt)} / N_0$ against BER of DCO-OFDM for 4-QAM, 16-QAM, 64-QAM and 256-QAM are plotted for a DC bias level of 7 dB and 13 dB respectively. $E\left\{x_{DCO(t)}\right\}$ is set to unity in all the graphs. An increase in the $E_{b(opt)} / N_0$ is also observed in these two plots both for the increased DC bias and higher order of constellations.

2.9.2 ACO-OFDM

Armstrong et al first proposed ACO-OFDM system in 2006. In an IM/DD ACO-OFDM system, only the odd subcarriers are used to carry data symbols. On the contrary, the even subcarriers are used to form a bias signal which ensures the non-negativity requirement of the transmitted signal.

The main difference of the ACO-OFDM transmitter is that there is no addition of DC bias as in a DCO-OFDM transmitter and the negative portions of the bipolar OFDM signal is clipped at zero which induces some clipping noise in the even subcarriers.

Just like the DCO-OFDM transmitter, x is serial to parallel converted, a CP is appended, Digital to Analog converted and filtered producing the signal, $x(t)$. Next, the negative signal value clipping at zero results in $x_{ACO(t)}$. Clipping at zero doesn't result in a loss of information as x has the property of anti-symmetry. The ACO-OFDM receiver processing is similar to the DCO-OFDM receiver; the only difference is that in ACO-OFDM, only the odd subcarriers are demodulated at the receiver, as only they carry data symbols.

2.9.2.1 ACO-OFDM Transmitter and Receiver

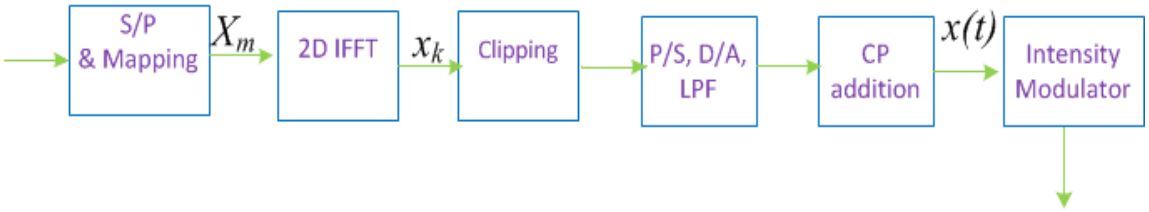

Figure 2-10 Block Diagram of an ACO-OFDM Transmitter

In *Figure 2-10*, the input signal to the IFFT block in the ACO-OFDM transmitter is first converted from serial to parallel and mapped onto the required constellation points. After this process, the input signal to the IFFT is, $X_m = \left[0, X_{m,1}, 0, X_{m,3,}, \ldots\ldots, X_{m,N-1}\right]$ where only the odd subcarriers are used to carry the data symbols. Just like the DCO-OFDM transmitter, in the ACO-OFDM transmitter, X_m is also constrained to have Hermitian symmetry. This process results in a real time signal x_k. In *Figure 2-11*, it is seen that, for every positive signal value, a negative counterpart is present at a distance of $N/2$. The clipped signal is shown in *Figure 2-12*. So it can be concluded that the signals should possess the anti-symmetry property in the time domain for maintaining Hermitian symmetry where the condition below is met.

$$x_k = -x_{k+N/2} \quad for \quad 0 < k < \frac{N}{2} \tag{2.6}$$

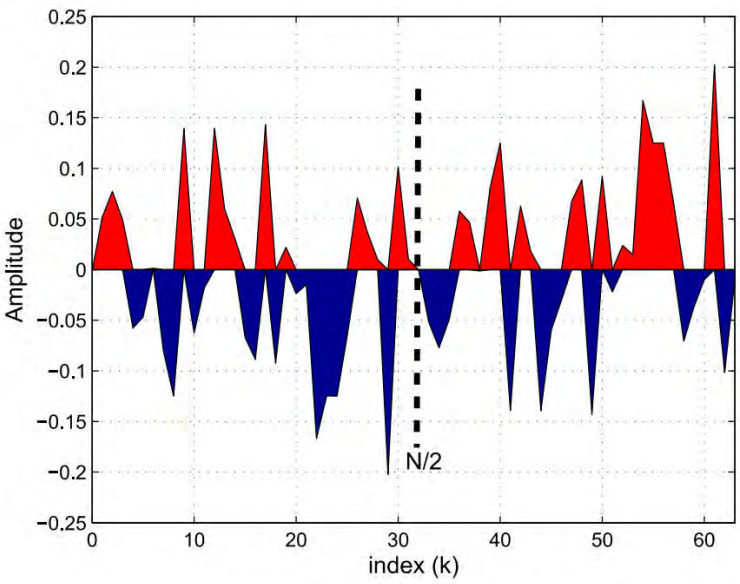

Figure 2-11 The output signal from the IFFT, x_k [22]

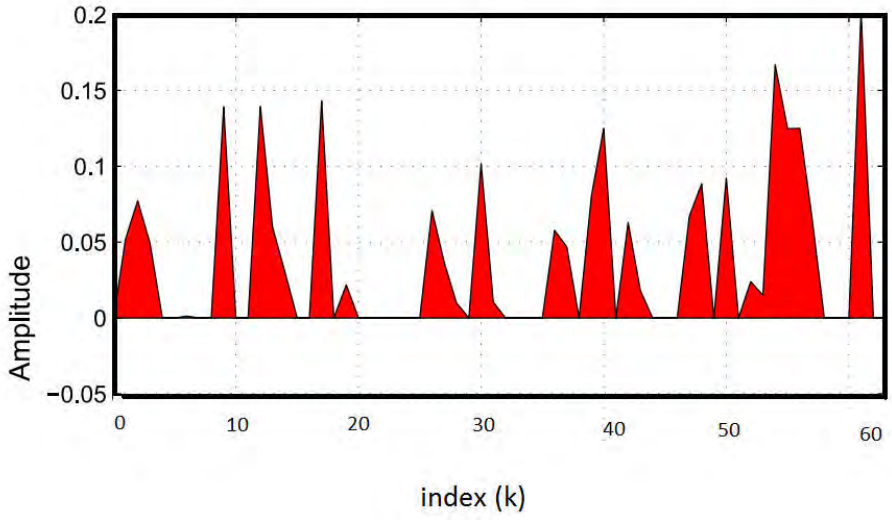

Figure 2-12 Transmitted signal [22]

2.9.2.2 ACO-OFDM Clipping Process

The whole ACO-OFDM clipping process is described like this: the clipping process makes the amplitude on the odd subcarriers half and a noise like interference appears on

the even subcarriers. For a better understanding of how x is affected by the zero biased clipping, the DFT of x is considered, where

$$X_m = \sum_{k=0}^{N-1} x_k \exp\left(\frac{-j2\pi km}{N}\right) \tag{2.7}$$

Separating out the positive and negative values of x_k , X_m can be expressed as follows,

$$\begin{aligned} X_m = & \sum_{k=0,x_{k>0}}^{\frac{N}{2}-1} x_k e\left(\frac{-j2\pi km}{N}\right) + \sum_{k=0,x_{k>0}}^{\frac{N}{2}-1} x_{k+\frac{N}{2}} e\left(\frac{-j2\pi\left(k+\frac{N}{2}\right)m}{N}\right) \\ & + \sum_{k=0,x_{k<0}}^{\frac{N}{2}-1} x_k e\left(\frac{-j2\pi km}{N}\right) + \sum_{k=0,x_{k<0}}^{\frac{N}{2}-1} x_{k+\frac{N}{2}} e\left(\frac{-j2\pi\left(k+\frac{N}{2}\right)m}{N}\right) \end{aligned} \tag{2.8}$$

Due to the anti-symmetry it can be expressed as:

$$\begin{aligned} X_m = & \sum_{k=0,x_{k>0}}^{\frac{N}{2}-1} x_k e\left(\frac{-j2\pi km}{N}\right) + \sum_{k=0,x_k>0}^{\frac{N}{2}-1} -x_{k+\frac{N}{2}} (-1)^m e\left(\frac{-j2\pi km}{N}\right) \\ & + \sum_{k=0,x_{k<0}}^{\frac{N}{2}-1} x_k e\left(\frac{-j2\pi km}{N}\right) + \sum_{k=0,x_k<0}^{\frac{N}{2}-1} -x_k (-1)^m e\left(\frac{-j2\pi km}{N}\right) \end{aligned} \tag{2.9}$$

As only the odd subcarriers are used to carry data symbols in ACO-OFDM, m is odd. Therefore,

$$X_m = 2\sum_{k=0,x_k>0}^{\frac{N}{2}-1} x_k e\left(\frac{-j2\pi km}{N}\right) + 2\sum_{k=0,x_k<0}^{\frac{N}{2}-1} x_k e\left(\frac{-j2\pi km}{N}\right) \tag{2.10}$$

After the clipping process is performed to produce $x_{ACO\ (t)}$, only the positive portion remains while the negative portion is clipped. After the DFT of $x_{ACO(t)}$ is taken, it is seen that

$$X_{ACO,m} = \frac{X_m}{2} + N_{ACO,m} \tag{2.11}$$

Where, the m^{th} element of the DFT vector of $x_{ACO(t)}$ is defined by $X_{ACO,m}$ and the m^{th} element of ACO-OFDM clipping noise vector is denoted by $N_{ACO,m}$. The ACO-OFDM clipping makes the value of X_m half which results in $X_m / 2$ to remain on odd frequencies and the remaining half just falls on the even subcarriers. The most surprising fact is that the information contained in $N_{ACO,m}$ is also very useful which is properly utilized in Diversity-combined ACO-OFDM.

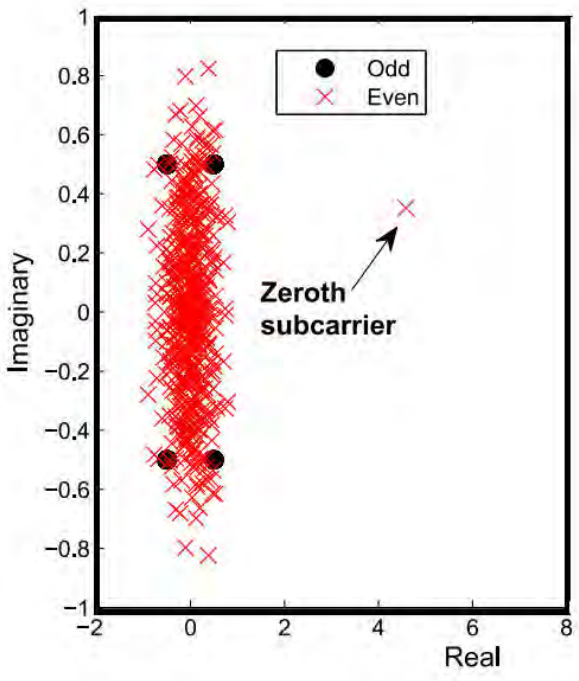

Figure 2-13 The constellation of the ACO-OFDM signal [22]

In *Figure 2-13*, the odd subcarriers and the even subcarriers are represented by black dots and red crosses respectively. The resultant signal on the even subcarriers is actually the ACO-OFDM clipping noise as no data symbols are transmitted on the even subcarriers at the transmitter side and it has to be kept in mind that the zeroth subcarrier has a large DC value.

2.9.2.3 Statistics and Performance of an ACO-OFDM System

The optical power of ACO-OFDM which is represented by $P_{opt,ACO}$ is,

$$P_{opt,ACO} = E\left\{x_{ACO}(t)\right\} = \int_0^\infty a f_{xACO(t)}(a)\,da = \frac{\sigma_A}{\sqrt{2\pi}} \tag{2.12}$$

Where σ_A is the standard deviation of the unclipped signal and $\sigma_A^2 = E\left\{x_k^2\right\}$.

The electrical power of ACO-OFDM is represented by $P_{elec,ACO}$ is given by,

$$P_{\text{elec},ACO} = E\left\{x^2{}_{ACO}(t)\right\} = \int_0^\infty a^2 f_{xACO(t)}(a)\,da = \frac{\sigma_A{}^2}{2} \tag{2.13}$$

And the relationship between these two is

$$E\left\{x_{ACO}(t)\right\} = \frac{\sqrt{E\left\{x^2{}_{ACO}(t)\right\}}}{\sqrt{\pi}} \tag{2.14}$$

The ratio of $E\left\{x_{ACO}(t)\right\}$ and $E\left\{x_{ACO}^2(t)\right\}$ depends on the level of optical power on $P_{opt,ACO}$. For avoiding the complexity of the calculation, $P_{opt,ACO} = 1$ has been assumed.

$$\frac{E\left\{x_{ACO}(t)\right\}}{b_{ACO}N_0} = \frac{1}{\pi}\frac{E\left\{x^2{}_{ACO}(t)\right\}}{b_{ACO}N_0} \tag{2.15}$$

Here, b_{ACO} is the bit rate of ACO-OFDM. $E\{x_{ACO}(t)\}/b_{ACO}N_0$ is the $E_{b(opt)}/N_0$ for ACO-OFDM and $E\{x^2{}_{ACO}(t)\}/b_{ACO}N_0$ is the $E_{b(elec)}/N_0$ for ACO-OFDM.

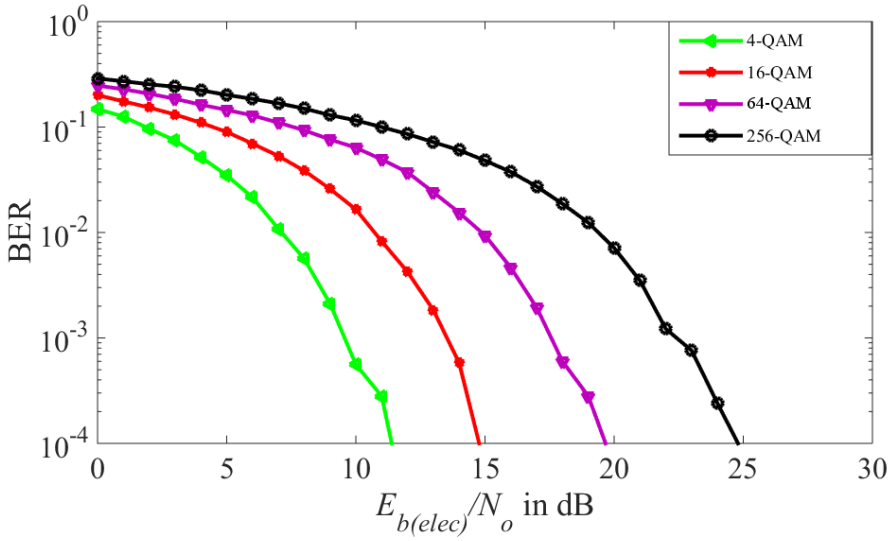

Figure 2-14 BER against $E_{b(elec)}/N_0$ of ACO-OFDM for 4-QAM, 16-QAM, 64-QAM and 256-QAM

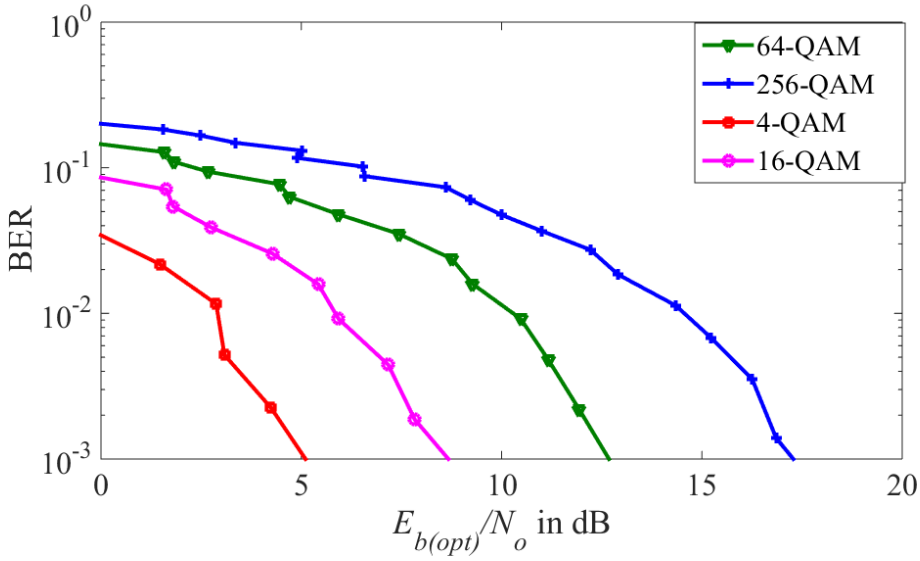

Figure 2-15 BER against $E_{b(opt)}/N_0$ for ACO-OFDM for 4-QAM, 16-QAM, 64-QAM and 256-QAM

The BER curves against $E_{b(elec)}/N_0$ and $E_{b(opt)}/N_0$ of ACO-OFDM for 4-QAM, 16-QAM, 64-QAM and 256-QAM have been demonstrated in *Figure 2-14* and *Figure 2-15*. The relationship between $E_{b(elec)}/N_0$ and $E_{b(opt)}/N_0$ is used for plotting this graph. The ACO-OFDM clipping is the reason for half of the power of the transmitted signal to fall on the even subcarriers and half of the power to remain on the odd subcarriers as well as to be utilized. During the detection process, only the odd subcarriers are utilized to carry the data symbols; therefore the performance of ACO-OFDM is 3 dB worse than the conventional OFDM counterpart like DCO-OFDM while considering spectral efficiency.

2.9.3 Diversity Combined ACO-OFDM

ACO-OFDM and DCO-OFDM are two modulation schemes that are applied in real time scenarios to transmit real, positive signals in an IM/DD system. Both of the schemes have their specific advantages and disadvantages as well. ACO-OFDM is more efficient in terms of optical power than DCO-OFDM for small constellations such as 4-QAM, 16-QAM, 64-QAM and 256-QAM but ACO-OFDM shows better efficiency than DCO-OFDM in case of large constellations such as 1024-QAM. A new technique combining the advantages of both of these techniques have been improvised namely Diversity Combined ACO-OFDM which shows better performance than the previously mentioned conventional schemes. It shows a gain of up to 3 dB in terms of electrical power. The theoretical gain of diversity-combined ACO-OFDM may not be attainable though in practical systems, due to noise and distortion in the lowest frequency, zeroth subcarrier.

2.9.3.1 Diversity Combined ACO-OFDM Transmitter

The transmitter of a Diversity Combined ACO-OFDM system is quite identical to a conventional ACO-OFDM transmitter. In a conventional ACO-OFDM transmitter, only the odd subcarriers are used to carry the data symbols. Therefore, demodulation is performed only on the odd subcarriers at the receiver side. But unlike an ACO-OFDM receiver, in a diversity combined ACO-OFDM receiver, demodulation is applied on both the odd and even subcarriers. The signals on the even subcarriers are then recovered after a non-linear process and they are combined with the signal on the odd subcarriers with a

weighting factor and flipping them with the help of the sign of the odd signal. This whole process results in a performance gain of up to 3 dB in electrical power.

2.9.3.2 Diversity Combined ACO-OFDM Receiver

The main components of a Diversity Combined ACO-OFDM receiver are: an optical to electrical converter such as a photodiode, an LPF, an (Analog to Digital) A/D converter and an (Serial to Parallel) S/P module. The data symbols are then sent through an FFT to convert the signal from discrete time domain to discrete time domain after being mapped onto the constellation points. The FFT signal output Y, is then equalized to remove the channel effects and distortion. The diversity combined ACO-OFDM receiver is similar to an ACO-OFDM receiver up to this point. In the next stage, the signal output in the frequency domain from the equalizer is separated into odd and even component vectors namely Y_{odd} and Y_{even}, where $Y_{odd} = \left[0, Y_1, 0, .., 0, Y_{N-1}\right]$ and $Y_{even} = \left[Y_0, 0, Y_2, ., Y_{N-2}, 0\right]$. Next, Y_{odd} and Y_{even} are input into two separate IFFTs and the resulting discrete time domain vectors are y_{odd} and y_{even} where $y_{odd} = \left[y_{odd,0,}.....,y_{odd,N-1}\right]$ and $y_{even} = \left[y_{even,0,}.....,y_{even,N-1}\right]$. The k^{th} element of y_{odd} is given by $y_{odd,k}$, where

$$y_{odd,k} = x'_{odd,k} + n_{odd,k} \tag{2.16}$$

$x'_{odd,k}$ is a component of x'_{odd} and x'_{odd} is the odd component of the transmitted discrete time domain signal x_{ACO} and $n_{odd,k}$ is an element of n_{odd} which is the odd component of the AWGN vector. $x'_{odd,k} = 0.5x_k$.

The k^{th} element of y_{even} is given by $y_{even,k}$, where

$$y_{even,k} = x'_{even,k} + n_{even,k} \tag{2.17}$$

$x'_{even,k}$ is an element of x'_{even} which is the even component of the transmitted discrete time vector, x_{ACO} and $n_{even,k}$ is the k^{th} element of n_{even} which is the even component of

the AWGN vector. $x'_{even,k} = 0.5|x_k|$ and it is evident that it is a unipolar signal. That is the reason for the non-linearly processing before being combined with the bipolar signal $x'_{odd,k}$. The processing of the even components depends on the relationship between odd and even signals of the following equation:

$$x'_{odd,k} = \text{sgn}\left(x'_{odd,k}\right) \times x'_{even,k} \tag{2.18}$$

$\text{sgn}\left(x'_{odd,k}\right)$ represents the sign of $x'_{odd,k}$. The equations imply that x'_{even} contains some information about the transmitted data which is ignored or clipped in a conventional ACO-OFDM system. The unipolar signal $x'_{even,k}$ is converted to a bipolar signal by multiplying it by the polarity of $x'_{odd,k}$ that is denoted by $\text{sgn}\left(x'_{odd,k}\right)$.

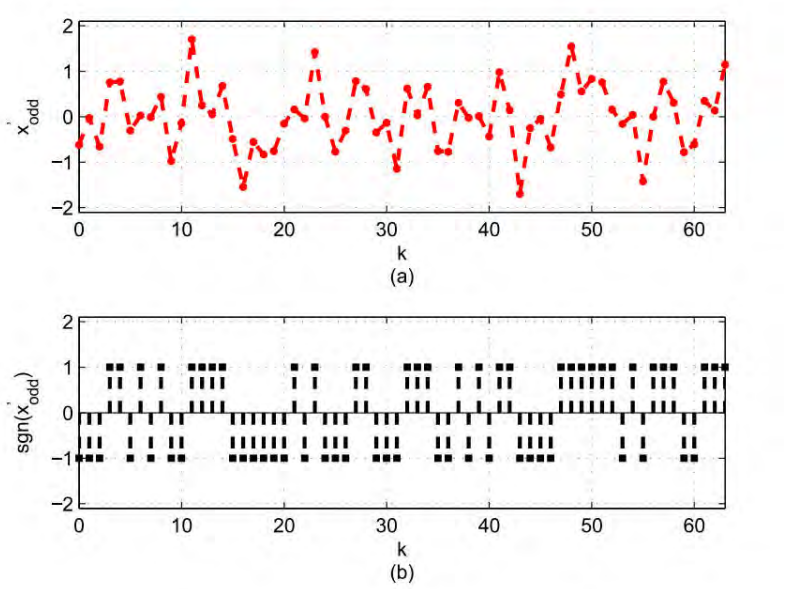

Figure 2-16 (a) Signal $x'_{odd,k}$ and Signal $\text{sgn}\left(x'_{odd}\right) \times x'_{even}$

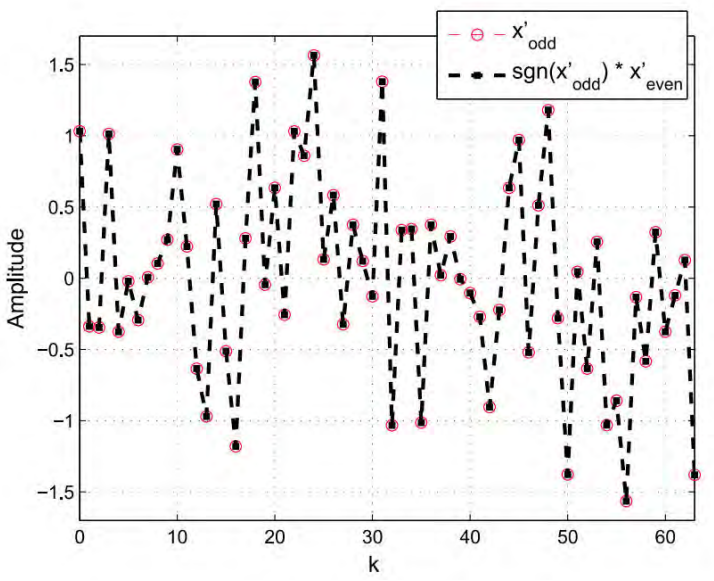

Figure 2-17 Signal x'_{odd} and signal $\mathrm{sgn}\left(x'_{odd}\right)\times x'_{even}$

In *Figure 2-16*, x'_{odd} and $\mathrm{sgn}\left(x'_{odd}\right)$ are shown separately and in *Figure 2-17*, both of them are plotted together in an intention to demonstrate that the signals fall on top of each other when plotted together. Hence, it is obvious that the non-linear operation, $\mathrm{sgn}\left(x'_{odd}\right)\times x'_{even}$ results in the same signal as x'_{odd} in the absence of any channel impairment. Corresponding to the fact, the non-linear processing operated on y_{even} is given by,

$$y'_{even,k} = \mathrm{sgn}\left(y_{odd,k}\right)\times y_{even,k} \tag{2.19}$$

The odd and even components are then combined using a weighting factor α :

$$y'_k = (1-\alpha)\, y_{odd,k} + \alpha y'_{even,k}, \quad 0 \le \alpha \le 1. \tag{2.20}$$

The value α is close to 0.5 for maximizing the highest gain. y'_k is converted back to the discrete frequency domain from the time domain through the FFT block and the transmitted data is recovered through proper signal processing. Spectral power efficiency is improved utilizing the information dormant in the even subcarriers and electrical

power efficiency also is improved already as it is a version of ACO-OFDM, where no additional DC bias is needed.

A comparatively better performance can be achieved by diversity combined ACO-OFDM incorporating genie case. In a genie case, the receiver has perfect assumption about which samples to invert at the stage of non-linear processing in the Diversity-Combined ACO-OFDM receiver. In a conventional diversity combining receiver, mere estimates of $\mathrm{sgn}\left(x'_{odd,k}\right)$ are used in processing the even frequency components whereas the exact values of $\mathrm{sgn}\left(x'_{odd,k}\right)$ are used in a genie diversity combining receiver.

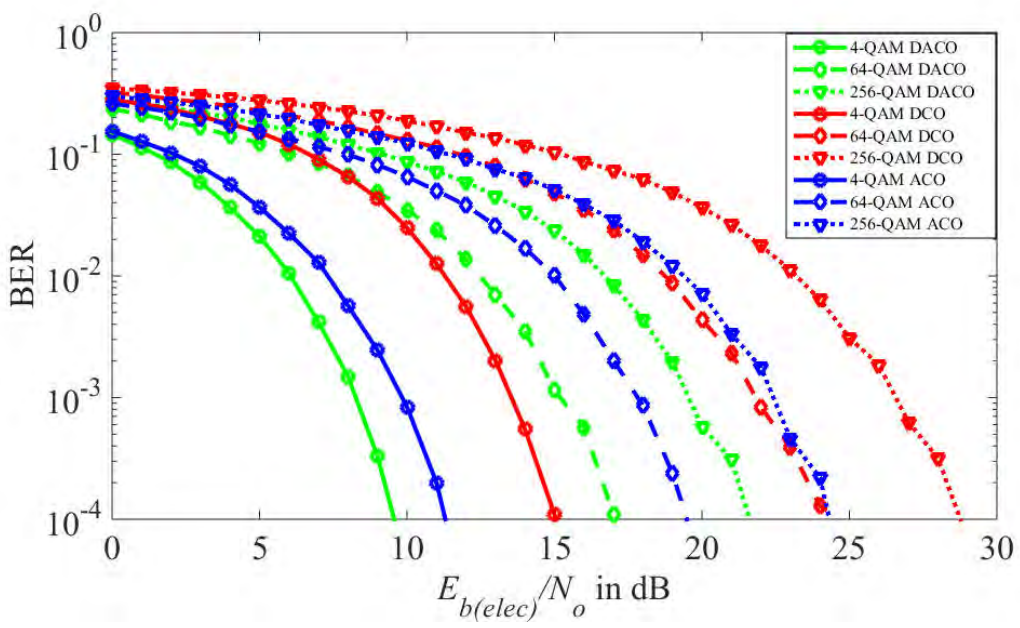

Figure 2-18 BER against $E_{b(elec)} / N_0$ for ACO-OFDM, ACO-OFDM and diversity-combined ACO-OFDM for 4-QAM, 64-QAM and 256-QAM constellations, with α=0.5

The BER against $E_{b(elec)} / N_0$ of DCO-OFDM, ACO-OFDM and Diversity-Combined ACO-OFDM for 4-QAM, 64-QAM and 256-QAM constellations have been shown in *Figure 2-18*. $\alpha = 0.5$ is used as the weighting factor for diversity-combined ACO-OFDM. It is obvious from the figure that DCO-OFDM performs better for lower frequencies and worst in higher frequencies. On the contrary, ACO-OFDM performs the

best as we increase the number of bits for the improvement of spectral efficiency and exhibits better Bit Error Rate performance. DACO-OFDM is even better at lower frequencies than ACO-OFDM and shows a bit worse performance than ACO-OFDM for higher frequencies.

The performance of DACO-OFDM has been demonstrated with the help of the plotted figures below:

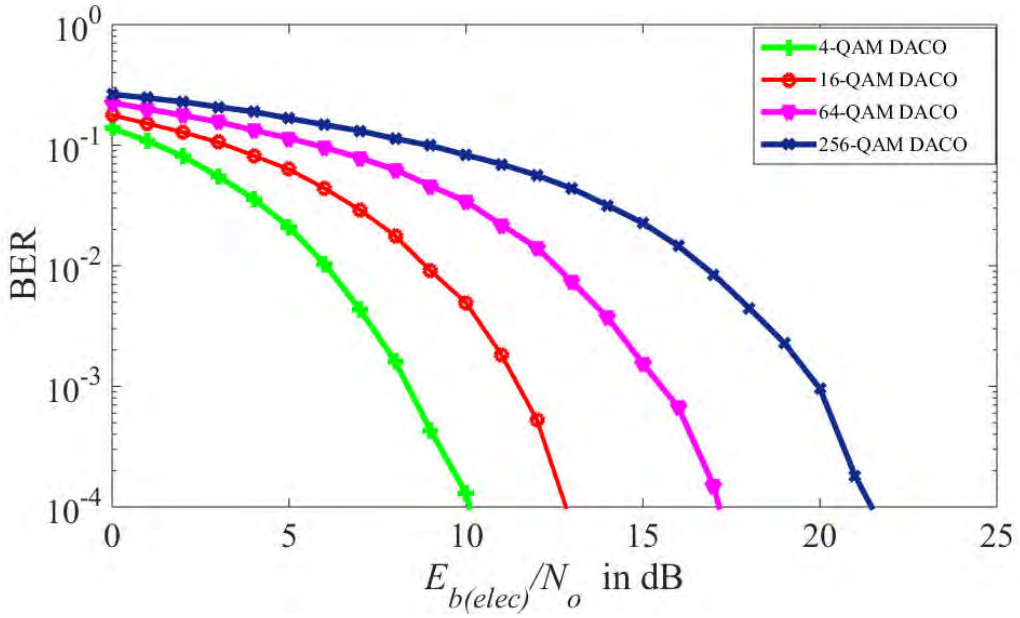

Figure 2-19 BER against $E_{b(elec)}/N_0$ for DACO-OFDM for 4-QAM, 16-QAM, 64-QAM and 256-QAM

BER versus $E_{b(elec)}/N_0$ has been plotted in *Figure 2-19* to show that in case of Diversity Combined ACO-OFDM, the electrical energy per bit increases for the same BER if we keep increasing the constellations. Because the higher constellations will add to more noise and will lead to more energy.

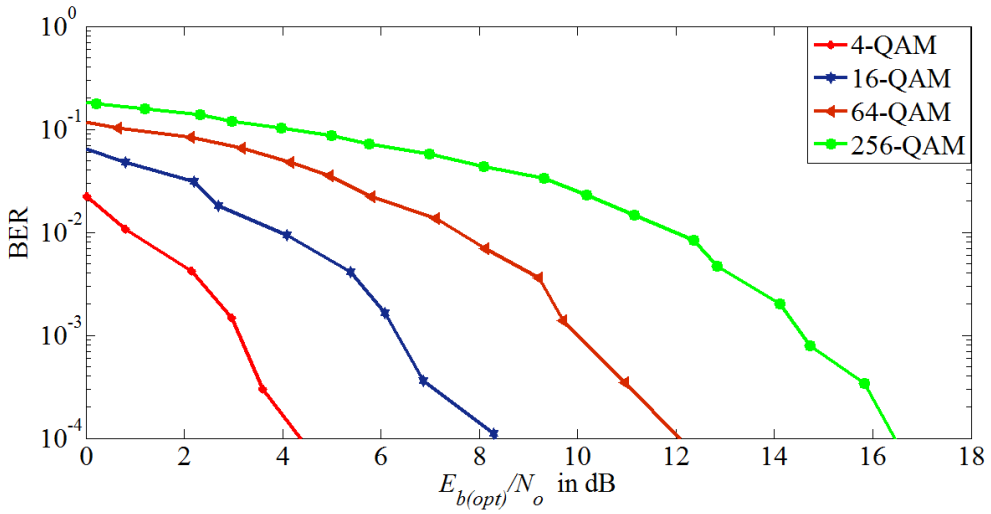

Figure 2-20 BER against $E_{b(opt)}/N_0$ for DACO-OFDM for 4-QAM, 16-QAM and 64-QAM

In the Figure 2-20 above, the performance of DACO-OFDM is shown in case of optical energy. BER versus $E_{b(opt)}/N_0$ proves that, for lower constellations, the system is very efficient as it requires a small optical energy but the performance will worsen to a greater degree in case of higher constellations.

2.9.3.3 Practical Limitations of Diversity-combined ACO-OFDM

From theoretical point of view, a gain of maximum 3 dB is possible in a diversity-combined ACO-OFDM system. But it's not achievable in practical scenario because the technique is extremely sensitive to noise and distortion in the lowest frequency. The DC offset present in the zeroth frequency subcarrier also increases the noise power to an extent. The biasing of the transmitter LED and the receiver photodiode circuit can cause the DC offset. Ambient light sources can also introduce DC offset in a practical optical wireless system. Low frequency attenuation can be introduced by the low pass nature of the front-ends of typical transmitters and receivers, the presence of incandescent and fluorescent lights.

The analysis of the implication of the zeroth subcarrier variations is as follows. The even component of the received signal $y_{even,k}$, is given by

$$y_{even,k} = x'_{even,k} + n_{even,k} + d_0, \tag{2.21}$$

Here, d_0 is the DC-offset. When $y_{even,k}$ is non-linearly processed, $y'_{even,k}$ is given by,

$$y'_{even,k} = \text{sgn}\left(y_{odd,k}\right) \times \left(x'_{even,k} + n_{even,k} + d_0\right) \tag{2.22}$$

In the absence of noise and distortion, $y'_{even,k} = x'_{odd,k}$. There are three possible sources of error such as DC offset, the AWGN, errors that occur when $\text{sgn}\left(y_{odd,k}\right) \neq \text{sgn}\left(x'_{odd,k}\right)$. But, only the bit errors due to $\text{sgn}\left(y_{odd,k}\right) \neq \text{sgn}\left(x'_{odd,k}\right)$ and AWGN are considered in the original diversity-combined system.

DC offsets will always be present and must be considered in a practical OWC system. The performance of diversity-combined ACO-OFDM is affected drastically in the presence of DC offset. The non-linear operation and the combining process also result in errors. The DC offset is quantified using the following equation:

$$D = 20\log_{10}\left(\frac{E\{x_{ACO}\} + d_0}{E\{x_{ACO}\}}\right) \tag{2.23}$$

2.9.4 ADO-OFDM

The ADO-OFDM is another modulation technique which has ACO-OFDM component on the odd subcarriers and the DCO-OFDM component on the even subcarriers. The detail technique is described in [22].

2.10 Summary

From the above discussions it has been observed that OWC has emerged as a solution to the existing problems associated with RF communication. Room illumination is now-a-days a lucrative feature to incorporate within indoor OWC while providing data communication by the same. OFDM is the most viable scheme for indoor OWC due to its robustness and high efficiency. Various IM/DD schemes have been adopted in order to make the bipolar signal unipolar. But Diversity Combined ACO-OFDM provides the best BER performance among all of them for it provides better spectral efficiency as well as better power efficiency.

CHAPTER 3

3 PREVIOUS RELATED WORKS

3.1 Overview

The related previous works have been discussed in this chapter. A new technique has been proposed in [51] based on using the signal on the odd frequency subcarriers which is termed as "DC odd frequency based estimation (DC-OFBE)". In [52], a simple combining algorithm is proposed with the help of a detailed analysis of NLCD (Non-Linear Clipping Distortion) which extracts the instructive information inside the clipping distortion and the process of recovering signal with zero-bias has also been shown there. Finally, in [53], a new receiver has been proposed for frequency domain diversity combining ACO-OFDM termed as FDCC and eFDCC receivers which have been proved superior to their other counterparts.

3.2 DC Odd Frequency Based Estimation in Diversity Combined ACO-OFDM

Normally, in an AWGN channel, ACO-OFDM outperforms DCO-OFDM for normalized bandwidth/bit rate greater than 0.2 and vice versa for smaller values. In previous works, it has been shown that ACO-OFDM gives an advantage of between 1.5dB and 4dB but it depends on how the comparison was made. But in another paper, DCO-OFDM gave better performance in their experimental configuration because of the capacitors in the receiver causing baseline wander leading to adverse effect on ACO-OFDM. Uncorrected DC offset in the receiver may be the reason of the failure of the diversity combined ACO-OFDM method, but DC correction methods can effectively address this problem.

Experimental results demonstrating the use of diversity combining in an optical wireless system using asymmetrically clipped optical orthogonal frequency division multiplexing (ACO-OFDM) are presented in [51]. An improvement of 2-3 dB has been shown by incorporating diversity combining in the experiments. As a transmitter, a standard white lighting LED of the type often used in visible light communication (VLC) is used.

3.2.1 Reasons for Incorporating DC-OFBE

Data is recovered from the odd frequencies only in the basic OFDM. But later it has been shown that the performance of ACO-OFDM could theoretically be improved by upto 3dB by dint of using diversity combining, which involves combining the signal received on the even subcarriers with the signal received on the odd ones. Knowledge of the zero level of received signal is assumed in case of diversity combining ACO-OFDM. Because normally, the use of optical transmission and the properties of the transmitter and the receiver imply that the zero level of the received signal might not correspond to the zero level of the transmitted electrical signal.

DC offset resulting due to the incorrect estimation of the zero level is the sole reason for diversity combining to fail. To overcome this problem, a new technique has been proposed in [51] based on using the signal on the odd frequency subcarriers. This is termed as “DC odd frequency based estimation (DC-OFBE)”. This process also reveals a new property and that is, unlike in an AWGN channel, the signal to noise ratio (SNR) improvement is frequency dependent. SNR improvement is nthe greatest on the most attenuated subcarriers.

In the receiver, two forms of diversity combining methods were implemented. It was shown that a direct application of the original diversity combining algorithm increased the SNR. DC offset resulting from the incorrect estimation of estimation of the zero level of the received signal, was mainly responsible for this. On the contrary, when DC offset was estimated using the odd frequency subcarriers, it resulted in a reduction of 2dB in the required SNR, for a bit error rate of 10^{-4} compared to ACO-OFDM alone.

One of the most important findings is that diversity combining alters the frequency distribution of noise in the equalized diversity-combined signal. This has been shown as a result of non-linear processing of even subcarriers in the diversity combining process. Consequently, diversity combining affects SNR on different subcarriers in different ways when applied in a frequency selective channel; i.e., the most attenuated subcarriers are faced with the greatest SNR increase.

3.2.2 Description of the Total Set-up and the DC-OFBE Process

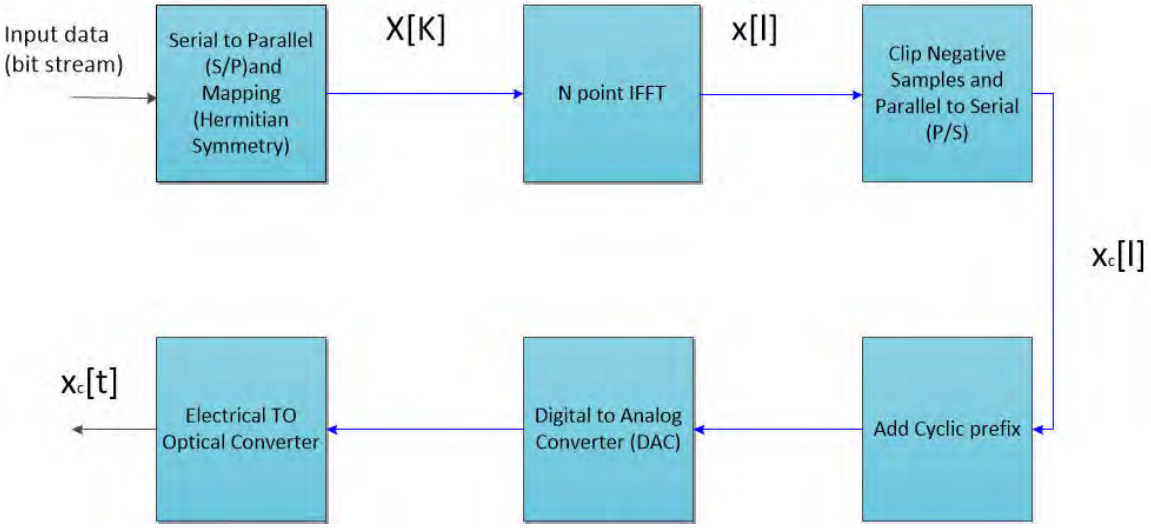

Figure 3-1 Block Diagram of an ACO-OFDM Transmitter

Figure 3-1 shows the block diagram of the transmitter used in [51]. The transmitted data is mapped onto the odd frequency subcarriers and the vector input to the inverse Fast Fourier Transform $X=\left[X\left[0\right],X\left[1\right],.....,X\left[N-1\right]\right]$. It is constrained to have Hermitian symmetry, i.e. $X\left[k\right]=X^{*}\left[N-k\right],0<k<N/2$, which ensures that outputs of the IFFT will be real.

The even frequency subcarriers are zero which means that only $N/4$ of the N complex inputs to the IFFT are independent. The signal is converted from the discrete

frequency domain to the discrete time domain by the IFFT. The IFFT output signal is clipped at zero to give the unipolar signal $x_c = \left[x_c[0], ..., x_c[N-1]\right]$ required for an IM/DD channel. And finally the data is input to a digital-to-analog converter (DAC) and converted into an optical signal, $x_c(t)$, using an LED after Cyclic Prefix addition.

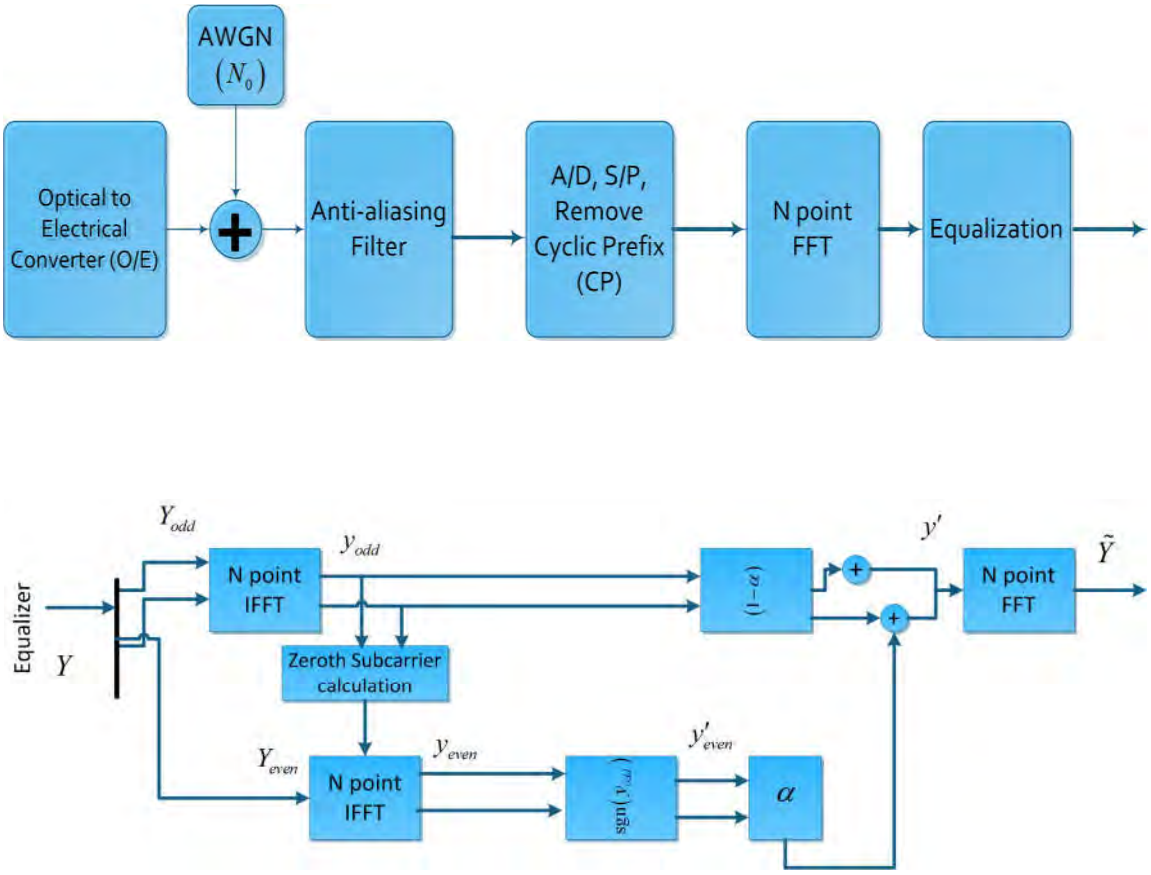

Figure 3-2 Block Diagram of the Diversity Combining Receiver with DC odd frequency based estimation

In *Figure 3-2*, an ACO-OFDM receiver using diversity-combining and DC-OFBE is shown. The first five blocks are just the same as a conventional ACO-OFDM receiver. But instead of recovering the data using the equalized symbol vector Y, further processing is done on this vector to recover the information carried on the even subcarriers. Y is separated into two vectors namely odd and even subcarriers, Y_{odd} and

Y_{even} respectively. Y_{odd} is input to the upper IFFT the outputs of which can be expressed as $y_{odd} = \left[y_{odd}[0], y_{odd}[1], ..., y_{odd}[N-1] \right]$ are then used for DC-OFBE to provide the estimate of the DC component, $\hat{Y}[0]$, given by:

$$\hat{Y}[0] = \sum_{l=0}^{N-1} | y_{odd}[l] | \tag{2.24}$$

The input to the lower IFFT is Y_{even} with the zeroth subcarrier substituted with $\hat{Y}[0]$. The output of this block is y_{even}. In order to recreate a bipolar signal y'_{even}, the absolute value of the output of the lower IFFT is then multiplied by the sign of the signal, y_{odd}. The combined signal y' is finally obtained by this formula:

$$y' = (1-\alpha) y_{odd} + \alpha y'_{even} \tag{2.25}$$

where α is a constant. A final FFT is performed to give $\tilde{Y}$ and the data is recovered from $\tilde{Y}$.

3.2.3 Experiments and Results

3.2.3.1 The Channel Frequency Response

The results of the experiment were analyzed utilizing the combination of measurements and simulation to derive the measured channel frequency response, the measured SNR for each subcarrier and the simulated BER curves based on the measured frequency

response because of the practical limitations of optical wireless experiments.

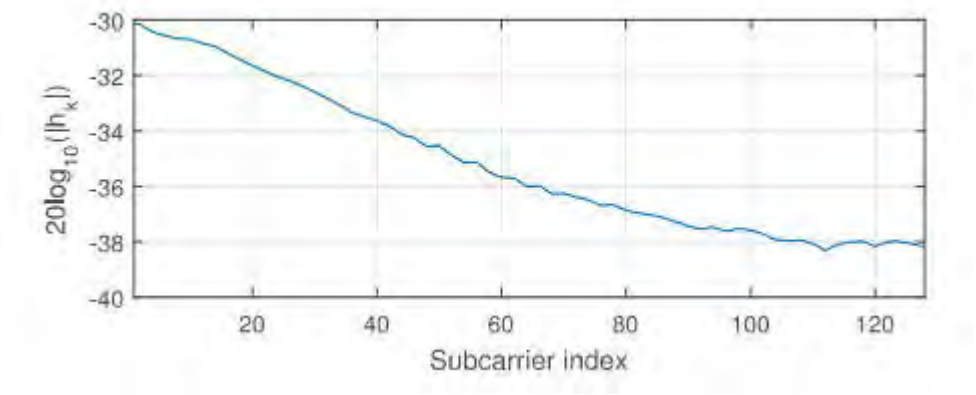

Figure 3-3 The measured channel frequency response [51]

The measured channel frequency response is shown in *Figure 3-3*. It can be seen that the channel gain drops as the frequency increases. Values for frequencies upto 10 MHz has been shown where h_k is the ratio of the received value on the k^{th} subcarrier before equalization, $Y_{rec}[k]$, to the transmitted value, $X_c[k]$, on the corresponding subcarrier after clipping, where $X_c = [X_c[0], X_c[1], ..., X_c[N-1]]$ is the FFT of signal x_c . All the values of h_k were calculated using

$$h_k = \frac{1}{N_{sym}} \sum_{j=1}^{N_{sym}} \frac{Y_{rec,j}[k]}{X_{c,j}[k]} \tag{2.26}$$

Here the subscript, j, denotes the index of the transmitted/received OFDM symbols. Much greater fluctuations were found in the estimated values for the even subcarriers than the odd ones. Low signal power on all except the zeroth even subcarrier is the sole reason of this. Linear interpolation between the adjacent odd subcarriers helped obtaining a more consistent result and by estimating h_k for the even subcarriers. The low pass characteristic of the frequency response is due to the combined effect of the blue LED surrounded by a phosphor coating used in the experiment.

3.2.3.2 Analysis of the Receiver SNR

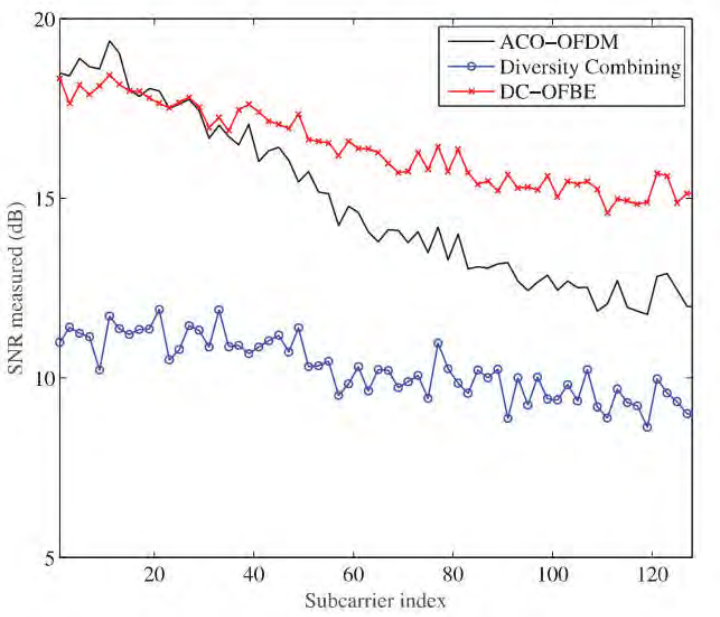

Figure 3-4 Experimental SNR versus subcarrier index [51]

Figure 3-4 shows the receiver SNR for each subcarrier as a function of subcarrier index in case of data carrying odd subcarriers. Averaging over the values measured for each of the 200 symbols, the SNR on each of the odd subcarriers was calculated. Three curves correspond to ACO-OFDM with no diversity combining, ACO-OFDM with diversity combining and ACO-OFDM with diversity combining and DC offset estimation. $\alpha = 0.5$ has been assumed here as this is close to the optimum value for high SNR. If there are no decoding errors, y_{odd} and y'_{even} have the same SNR and assuming $\alpha = 0.5$ makes them contribute equally to y'.

As per expectation, the ACO-OFDM results decrease with frequency with a 2 dB drop over the 10 MHz bandwidth. Furthermore, baseline wander was not present in ACO-OFDM without diversity combining because of the design of the optical receiver. But, the SNR is between 5 and 10 dB worse than for simple ACO-OFDM when diversity combining is applied without DC offset estimation. On the other hand, applying DC-

OFBE along with diversity combining improves the performance significantly on most subcarriers.

From the experiment, it has been observed that for the lowest frequency subcarriers, diversity combining with DC-OFBE reduces rather than increases the SNR. Analysis of the noise power at various points in the receiver can give a good explanation of this phenomenon. As noise power is an increasing function of frequency, the channel response falls with increasing frequency. According to the sign of y_{odd}, the signal y_{even} is flipped. The flipped signal y'_{even} contains odd subcarriers only and the noise component is evenly distributed across the subcarriers. As the signal y'_{even} has higher noise power than y_{odd} on low frequencies but lower noise power on high frequencies, therefore, when combination of both of them results in a noise power which may exceed that of y_{odd}, leading to lower SNR than when odd subcarriers alone are used.

It is not possible to measure the variation in BER with $E_b(opt)/N_0$ experimentally. The transmitted optical power, the received level of AWGN also can't be measured and the level of AWGN cannot be varied in the experiment. The number of bits which can be transmitted is also limited by the memory of the AWGN.

3.2.3.3 Comparison among the Existing Systems

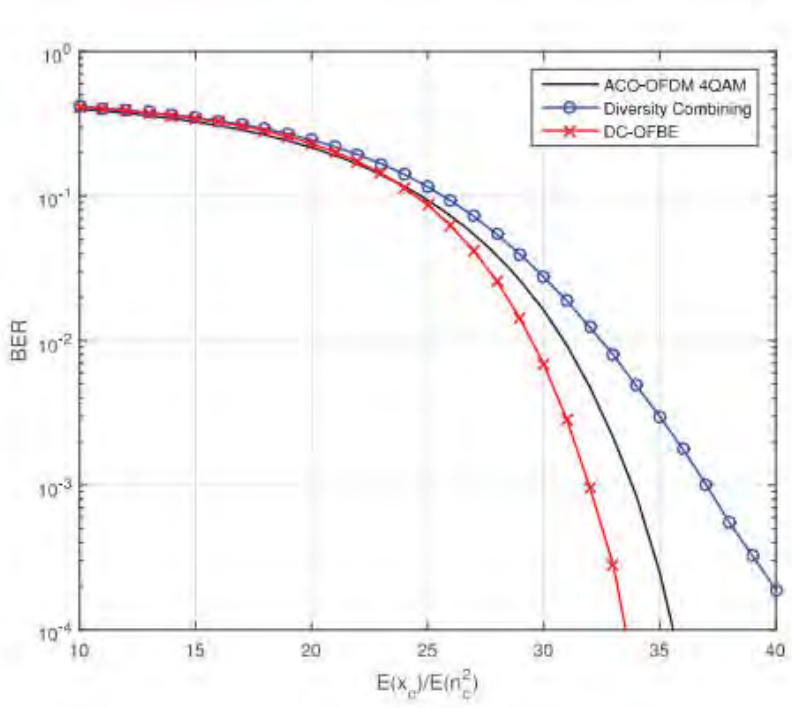

Figure 3-5 BER versus $E\{x_c\}/E\{n_c^2\}$ (in dB) in a frequency selective channel [51]

The BER curves shown in *Figure 3-5* are presented as a function of $E\{x_c\}/E\{n_c^2\}$. Here, $E\{n_c^2\}$ is the variance of the noise after the anti-aliasing filter and x_c is normalized so that $E\{x_c\}=1$. With the optical power normalized to unity which is often used in the theoretical work, this function is linearly related to the value $E_b(opt)/N_0$. The importance of accurate DC estimation has been shown in *Figure 3-5*. The use of the actual value of the zeroth subcarrier which includes the DC offset leads to worse performance than conventional ACO-OFDM. But when DC-OFBE is used, diversity combining results in a 2 dB improvement in performance at a BER of 10^{-4}.

3.2.4 Modifications for Improved performance

In the experiment conducted in [51], the transmitter and the receiver were separated by 2.5 cm. The off-the-shelf equipment as well as the simple design makes the experiment repeatable by other researchers. The distance could be increased in a number of ways by using custom-designed electronics in the transmitter and the receiver in a commercial implementation of VLC. Multiple LEDs could be driven in parallel in the transmitter for the purpose of increasing the power of the transmitted optical signal. In order to increase the received power, a larger area photodiode with a custom-designed amplifier could be used at the receiver. A separate anti-aliasing filter with a lower bandwidth could be used to reduce the noise in the received signal instead of depending on the low pass filtering which is incorporated in the DSO front-end. But all these changes are all in the domain of electronic design rather than in the domain of communication.

3.3 Diversity Combined ACO-OFDM with Zero-Bias and Utilizing NLCD on the Even Sub-Channels

3.3.1 The Underlying Reasons Behind this Process

The asymmetric clipping and associated biasing performed due to the unipolarity of the IM/DD channel result in a significant signal degradation. ACO-OFDM was proposed in order to overcome this detrimental distortion with the cost of a lower spectral efficiency. In [52], a simple combining algorithm is proposed with the help of a detailed analysis of such distortion which extracts the instructive information inside the clipping distortion. It is better compared to the aforementioned system because it applies zero-bias and reduces the clipping distortion to a great extent. The problem of performance enhancement for Orthogonal Frequency-Division Multiplexing (OFDM) transmission in intensity modulated, direct detected (IM/DD) optical systems is highlighted here. Neither any change to the existing optical plant nor any extra transmitting power is required. Thus, the receiver SNR can be significantly improved by exploiting the spectral diversity gain.

3.3.2 Main Objective of this Process

The objective of [52] is to develop an IM/DD optical OFDM system that makes a more efficient use of electronic power by means of electrical signal processing. At the transmitter, specially tailored signals with temporal diversity is generated and transmitted so that no electronic bias is needed. And at the receiver side, by means of combined decoding, the nonlinear clipping effect and the resulted spectral diversity can be effectively characterized so that the system performance can be improved.

3.3.3 The Constraints and Sensitivity to Non-Linear Distortion

Optical OFDM can be realized by two ways: by direct detection with appropriate electronic or optical biases or by coherent detection by dint of optical I/Q modulation. Very narrow linewidth lasers and sophisticated calibration algorithms are required in coherent systems due to the sensitivity of OFDM to frequency offsets and phase noise, as a trade-off for a superior performance.

On the other hand, direct detection provides simpler detection as well as minimum modification on existing plants with a lower power efficiency. Another fact should be kept in mind that, the transmission of such signal is largely restricted by the linearity constraints in the modulation/demodulation processes and the nonlinear effects created on the optical link. For the instantaneous envelope of an OFDM waveform can be approximated into a Gaussian distribution with a large peak-to-average power ratio (PAPR), optical OFDM is very sensitive to disturbances like non-linear distortion. The receiver signal-to-noise ratio is negatively affected by adding the large electronic bias in IM/DD optical OFDM transmission in order to avoid frequent clipping of negative peaks. By using only half of the subchannels, information can be recovered noiselessly with 0-bias clipping except for a power penalty. A combining decoding algorithm is proposed in [52] by utilizing the clipping-introduced spectral diversity at the receiver.

3.3.4 SNR Improvement by Applying Different Biases

In all the previous works, appropriate and variable DC offset has been added to eliminate all the clippings which calls for inspection or exhaustive search over data sequences. It is not favorable for systems with large number of sub-channels. Fixed yet large enough power has been applied in some works to ensure an infrequent clipping from a statistical point of view. But, it should be kept in mind that the maximum allowable input power for modulators and amplifiers is limited for any practical system.

Furthermore, a large electronic bias dramatically increases the power of the driving signal and Automatic Gain Control has to be used to shrink the power before using it into an optical modulator causing the receiver SNR to decrease after a certain biasing point. Therefore, an optimal biasing point exists for a practical system with a specific modulation format and receiver sensitivity for maximization of the performance.

An SNR improvement of 4 dB can be observed in “Opt-biased, Full rate”, compared to “Suff-Biased, Full rate”, which uses simple sufficient biases to eliminate all clippings. As a step to further improve the power efficiency, a new method has been improvised, where the bipolar signals can be recovered in absence of noise by using only odd subchannels, even without any bias. This is called the “Zero-Biased, half rate” system where half of the available bandwidth is simply abandoned at the receivers to eliminate the effect of non-linear clipping. This zero-biased system has a lower spectral/power efficiency but exhibits superior performance as effective rate is halved compared to other “Full rate” setups.

3.3.5 Temporal Diversity and 0-Bias Clipping

At the transmitter side, the data are first encoded into QAM symbols and applied onto N equally spaced sub-channels. Then the high speed data is first separated into a large number of low speed data sets by a serial to parallel converter. Afterwards, by the help of IFFT, the complex symbols are then transformed into a time domain signal and the k^{th} sample of the output is given by

$$x_k = \frac{1}{N}\sum_{m=0}^{N-1}(X_m^I + jX_m^Q)e(j\frac{2\pi}{N}km), \tag{2.27}$$

Here, the complex symbol modulated on the m^{th} sub-channel is $X_m = X_m^I + jX_m^Q$. For maintaining the Hermitian symmetry, $X_m^I = X_{N-m}^I$ and $X_m^Q = -X_{N-m}^Q$ for all m, except the first tone. The IFFT output will then be transformed into a digital data sequence x_k by a parallel-to-serial converter and converted from digital to analog waveform by a digital-to-analog converter. A biasing and clipping process is required for making the bipolar signal unipolar to make it suitable for the delivery through the IM/DD channel. If the biasing voltage is denoted by I_{DC} and the equivalent biased and clipped time-domain samples are denoted by x_k', which represents the output distorted signal sequence are:

$$x_k' = \begin{Bmatrix} 0, x_k < -I_{DC} \\ x_k + I_{DC}, x_k \geq -I_{DC} \end{Bmatrix} \tag{2.28}$$

This is the driving signal for the ideal optical modulator, where the output optical power is a replica of the electric-drive signal and dispersion is considered to be the only limiting factor for simplicity. Appropriate demodulation at the receiver side is assumed after the photodiode part.

During the IFFT modulation process, each time sample x_k can be thought of as a summation of N phase rotated QAM symbols from all sub-channels. And it has been shown earlier that, if only odd sub-channels are loaded with data, $x_k = x_{k,odd}$; an anti-periodic sequence. There exists a unique sample in the second half with the same amplitude but opposite sign for any sample point in the first half. However, the anti-periodic sequence can also be treated as the output of a virtual repetition encoder from a coding point of view, where the input signal is simply flipped and repeated. By a full $N/2$ point IFFT loaded with appropriate inputs, $N/2$ point, time-domain input signal for the encoder can be easily obtained. The transmission bandwidth is thus doubled after the encoding, for only 50% of the sub-channels are loaded. Hence, the presence of this

temporal diversity poses an interesting problem in case of utilizing the temporal diversity for effectively transmitting the data and demodulating it in different channel conditions.

For explaining the overall system, an ideal bipolar channel where there is no negative clipping is being considered. To denote the joint effect of various noise processes which may be present at the receiver side, a zero-mean Gaussian noise process e_k with variance σ^2 is used; $y_k = x_k + e_k$,where x_k is the transmitted anti-periodic signal and e_k is an independent stationary process with corresponding self-correlation function $R_{xx[N/2]} = 0$. Different versions of the same signal are independently received namely y_k and $y_{k+N/2}$. Generally, an optimal diversity gain is provided by maximum ratio combining with equal power coefficient. The received signal after the combining is:

$$\hat{y}_k = \begin{Bmatrix} \frac{1}{2}\left(y_k - y_{k+\frac{N}{2}} \right), k = 0,1,....,\frac{N}{2}-1 \\ \frac{1}{2}\left(y_k - y_{k-\frac{N}{2}} \right), k = \frac{N}{2},\frac{N}{2}+1,....,N-1 \end{Bmatrix} \tag{2.29}$$

After biasing and clipping in the unipolar IM/DD channel, all the negative sample points are replaced by 0's before being applied onto optical modulator. But, it has been shown that even with no electronic bias, i.e., (if I_{DC} is set to 0 in (2.28)), the anti-periodic signal can still be perfectly recovered in absence of noise, i.e., the clipping distortion can be avoided. It can be justified from an information theory point of view that although $N/2$ negative sample points are replaced by 0, their positive siblings will all survive. Exactly one copy of the original information can be preserved and therefore, there is no information loss in the transmission.

With a perfect channel estimation, the received data on a odd sub-channel, m with a perfect channel estimation and in absence of any noise and interference,

$$X'_m = \sum_{k=0}^{N-1} \lfloor x_k \rfloor_c \, e\left(-j\frac{2\pi}{N}km\right)$$
$$= \sum_{k=0}^{\frac{N}{2}-1} \lfloor x_k \rfloor_c \, e\left(-j\frac{2\pi}{N}km\right) + \sum_{k=0}^{\frac{N}{2}-1} \left\lfloor x_{k+\frac{N}{2}} \right\rfloor_c e\left(-j\frac{2\pi}{N}\left(k+\frac{N}{2}\right)m\right) \tag{2.30}$$

where $\lfloor . \rfloor_c$ denotes the operator for the 0-bias clipping.

The exp (.) terms in the second summation can be deduced to

$$e\left[-j\frac{2\pi}{N}\left(k+\frac{N}{2}\right)m\right] = -e\left(-j\frac{2\pi}{N}km\right) \tag{2.31}$$

$$X'_m = \sum_{k=0}^{N/2-1} \lfloor x_k \rfloor_c \, e\left(-j\frac{2\pi}{N}km\right) + \sum_{k=0}^{N/2-1} -\lfloor -x_k \rfloor_c \, e\left(-j\frac{2\pi}{N}km\right)$$
$$= \sum_{k=0}^{N/2-1} x_k e\left(-j\frac{2\pi}{N}km\right) \tag{2.32}$$

where

$$\lfloor -x_k \rfloor_c = -\left(x_k - \lfloor x_k \rfloor_c\right) \tag{2.33}$$

Using a similar approach, without any clipping, the received signal can be expressed as a normal FFT, $\Im(.)$, as x_k is anti-periodic:

$$X_m \triangleq \Im(x_k) = 2\sum_{k=0}^{N/2-1} x_k e\left(-j\frac{2\pi}{N}km\right) \tag{2.34}$$

Hence,

$$X'_m = \frac{1}{2}X_m \tag{2.35}$$

No clipping distortion will be present on any of those sub-channels even with 0 bias. Information on any odd sub-channel m can be perfectly recovered in the absence of

noise and interference, considering that there is a constant attenuation factor of 2 on the amplitude.

3.3.6 Clipping Distortion and Spectral Diversity

The signal power is halved after 0-bias clipping for any anti-periodic sequence x_k generated at the IFFT output when odd sub-channels are loaded.

$$\sum_{k=0}^{N-1}\left\lfloor x_k \right\rfloor_c^2 = \frac{1}{2}\sum_{k=0}^{N-1} x_k^2$$
$$\sum_{k=0}^{N-1} X'_m{}^2 = \frac{1}{4}\sum_{k=0}^{N-1} X_m{}^2 = \frac{1}{4}\sum_{k=0}^{N-1} x_k{}^2 = \frac{1}{2}\sum_{k=0}^{N-1}\left\lfloor x_k \right\rfloor_c^2 \tag{2.36}$$

Which means that only half of the transmitted power will be picked up for decoding. The other half, however, will leak into even sub-channels and would result in a nonlinear clipping distortion (NLCD). In previous works, this distortion was treated as clipping noise without careful characterization and simply discarded before the decoding phase. But this NLCD contains useful information about the signal which has been explained by dint of equations. Theoretical characterization of this NLCD and consequently, efficient ways of utilizing the NLCD are the main focus of [52] in order to explore the possibility of a higher power efficiency.

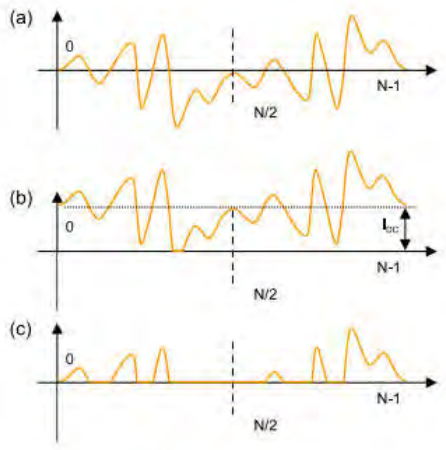

Figure 3-6 (a) An anti-periodic electronic OFDM waveform, (b) the corresponding biased and clipped signal, and (c) the corresponding 0-biased clipped signal. [52]

If a perfect channel is estimated, the resulting NLCD on an even sub-channel n after the 0-bias clipping and in the absence of any other noises and interferences is:

$$\begin{aligned} X'_n &= \sum_{k=0}^{N-1} \lfloor x_k \rfloor_c \, e\left(-j\frac{2\pi}{N}kn\right) \\ &= \sum_{k=0}^{N/2-1} \lfloor x_k \rfloor_c \, e\left(-j\frac{2\pi}{N}kn\right) + \sum_{k=0}^{N/2-1} \lfloor x_k \rfloor_c \, e\left(-j\frac{2\pi}{N}\left(k+N/2\right)n\right) \end{aligned} \tag{2.37}$$

As n is at least divisible by 2, all exp (.) phase shift terms are same, i.e.

$$e\left(-j\frac{2\pi}{N}\left(k+N/2\right)n\right) = e\left(-j\frac{2\pi}{N}kn\right) \tag{2.38}$$

$$\begin{aligned} X'_n &= \sum_{k=0}^{N/2-1} \left(\lfloor x_k \rfloor_c + \lfloor -x_k \rfloor_c\right) e\left(-j\frac{2\pi}{N}kn\right) \\ \text{So,} \quad &= \sum_{k=0}^{N/2-1} |x_k| e\left(-j\frac{2\pi}{N}kn\right) \\ &= \frac{1}{2}\Im\left(|x_k|\right) \end{aligned} \tag{2.39}$$

Therefore, in lieu of being treated as mere detrimental noises, the NLCD on even sub-channels actually contains instructive information about the transmitted signal and this information can be used to benefit the receiver SNR. In a nutshell, the resulting NLCD on even sub-channel n is $X'_n = \frac{1}{2}\Im\left(|x_k|\right)$, whereas decoded symbols on odd sub-channel m are:

$$X'_m = \frac{1}{2}\Im\left(x_k\right) \tag{2.40}$$

So, a combining decoding algorithm can be used to further improve the receiver SNR inspired by the MRC algorithm. Considering that the frequency-domain noise process W_m due to e_k has relatively low correlations among odd and even sub-channels, two

highly correlated signals $\left(x_k \text{ and } |x_k|\right)$ are virtually delivered through two reasonably independent channels, i.e.,

$$\begin{aligned} Y'_m &= X'_m + W_m \\ Y'_n &= X'_n + W_n \end{aligned} \tag{2.41}$$

An anti-periodic signal y_k^m, as well as a periodic signal $|y_k^n|$ can be regenerated by loading Y'_m and Y'_n to only the odd and even sub-channels of two separate IFFTs separately.

$$\begin{aligned} y_k^m &= \Im^{-1}\left(Y'_m\right) = \frac{1}{2}x_k + e_k^m \\ |y_k^n| &= \Im^{-1}\left(Y'_n\right) = \frac{1}{2}|x_k| + e_k^n \end{aligned} \tag{2.42}$$

Where the IFFT process is denoted by $\Im^{-1}(.)$, e_k^m and e_k^n are the corresponding time domain noises after the IFFT process. Furthermore, if we extract the polarity information of y_k^m and use it as the indicator of sign flipping on the even $|y_k^n|$ sequence, the reconstructed anti-periodic signal can be expressed :

$$\lceil y_k^n \rceil_r = \begin{cases} |y_k^n|, y_k^m \geq 0 \\ -|y_k^n|, y_k^m < 0 \end{cases} \tag{2.43}$$

Any incorrect sign flipping because of the noise process will lead to a corresponding error in $\lceil y_k^n \rceil_r$ as recovering $\lceil y_k^n \rceil_r$ calls for additional polarity information from the signal y_k^m . But the noise, which has an opposite polarity has to be way more larger than the corresponding signal for this error propagation to take place.

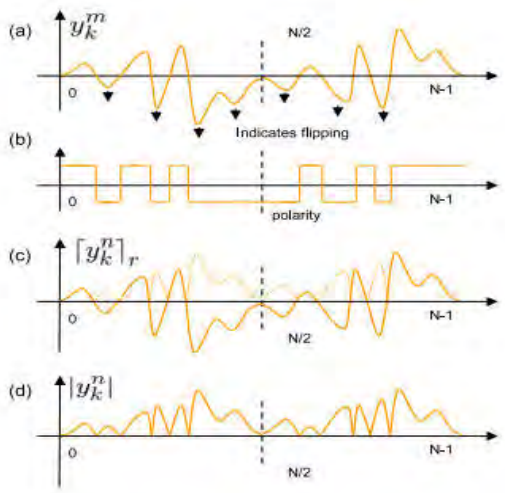

Figure 3-7 The recovery of $\lceil y_k^n \rceil_r$ from $|y_k^n|$ with the help of y_k^m sequence and its polarity [52]

So, those signal points with relatively small power are prone to errors mostly. Incorrect flipping of the same will cause only a marginal effect. On the contrary, a detrimental flipping large magnitude signal due to a very large noise is highly unlikely. That is the reason $\lceil y_k^n \rceil_r$ will suffer a small SNR penalty compared to y_k^m. The combined decoding equation incorporating the combining coefficient α (ranging from (0,1)), regenerated sign indicating signal y_k^m and reconstructed signal $\lceil y_k^n \rceil_r$ is :

$$\hat{y}_k = (1-\alpha)\, y_k^m + \alpha \lceil y_k^n \rceil_r \tag{2.44}$$

3.3.7 Performance Analysis

In [52], the performance of a simulated IM/DD optical OFDM system with 1024 sub-channels loaded with either 4-QAM or 16-QAM complex symbols has been analyzed. Losses and dispersions accumulated along the optical path are fully compensated and nonlinearities and ASE noise is not included as optical OFDM had shown a strong tolerance to both attenuation and dispersion. The presence of such channel effects would not create much disturbance as OFDM is indeed a multi-career scheme with lots of parallel sub-channels. As long as symbols on odd sub-channels are detectable,

information on even sub-channels are also explorable. However, a zero-mean Gaussian noise process is used to stimulate the joint effect of various noise processes at the receiver for simplicity.

When α is chosen to be around 0.45, the proposed algorithm provides an up to 2.53 dB higher SNR in case of small or medium receiver SNR; without any extra transmission power or transmission hardware. For example, the Symbol Error Rate (SER) curves for the system with combining decoding algorithm can provide a steady as well as increasing SNR gain upto 2.53 dB. Another noteworthy point is that the performance of a 16-QAM 0-biased ACO-OFDM system with combining decoding is better than a 4-QAM Opt-biased providing the same bit rate; for a medium SNR value around 13 dB. This feature makes it wise to trade spectral efficiency for a better performance which is an attractive feature for wireless optic or local transmission where the optical bandwidth is numerous. So, by dint of combining decoding, high power efficiency and a better performance are achievable at the same time with no extra cost of optical power or transmitter hardware.

3.4 The Best Receiver for ACO-OFDM Systems

In [53], a new receiver based on frequency-domain diversity combining (FDCC) for an asymmetrically clipped optical orthogonal frequency-division multiplexing (ACO-OFDM) system has been proposed. It is capable of exploiting the frequency selectivity of the channel more effectively to further improve the detection performance compared to its time-domain diversity combining (TDCC) counterpart, which is proved by postcombining signal-to-noise-ratio (SNR) analysis. An enhanced version of the FDCC receiver, which is called eFDCC, allowing for optimal selection among multiple sets of candidate symbol vectors based on signum matrix calculation, is also proposed [53]. The proposed FDCC and eFDCC receivers have been proved superior to the TDCC receiver through simulation results. The eFDCC receiver even performs better than an iterative receiver which is known to have superior performance in current literature. The complexity of the eFDCC receiver is also lower due to the avoidance of matrix

inversion. Hence, eFDCC as well as FDCC receivers are the best receivers for the ACO-OFDM system.

3.5 Summary

From the above discussions and analysis it is obvious that applying zero-bias to the transmitted signal will not only increase power efficiency but also will reduce the clipping noise. Moreover, this reduction is very important in diversity combined ACO-OFDM as the system is highly sensitive to non-linear clipping distortions. Secondly, the zeroth subcarrier DC Offset estimation with the help of signals on the odd subchannels also helps to improve the performance than rather estimating it. Finally, eFDCC receiver performs the best in case of frequency domain diversity combining ACO-OFDM, but it has not been considered in this thesis as the receiver in the time domain has been focused throughout the thesis. The next chapter combines the aspects of DACO-OFDM and DCO-OFDM to form a new modulation technique known as HDC-OFDM.

CHAPTER 4

4 PROPOSED HDC-OFDM

4.1 Overview

This chapter describes the proposed HDC-OFDM system and compares its performance with the existing optical OFDM schemes such as ACO-OFDM, DCO-OFDM, ADO-OFDM and DACO-OFDM.

4.2 Description of HDC-OFDM

It has already been mentioned that the proposed HDC-OFDM system is a combination of the ideas of DACO-OFDM and DCO-OFDM. A typical HDC-OFDM scheme is described in the following.

4.2.1 HDC-OFDM Transmitter

The transmitter of an HDC-OFDM system is shown in *Figure 4-1*:

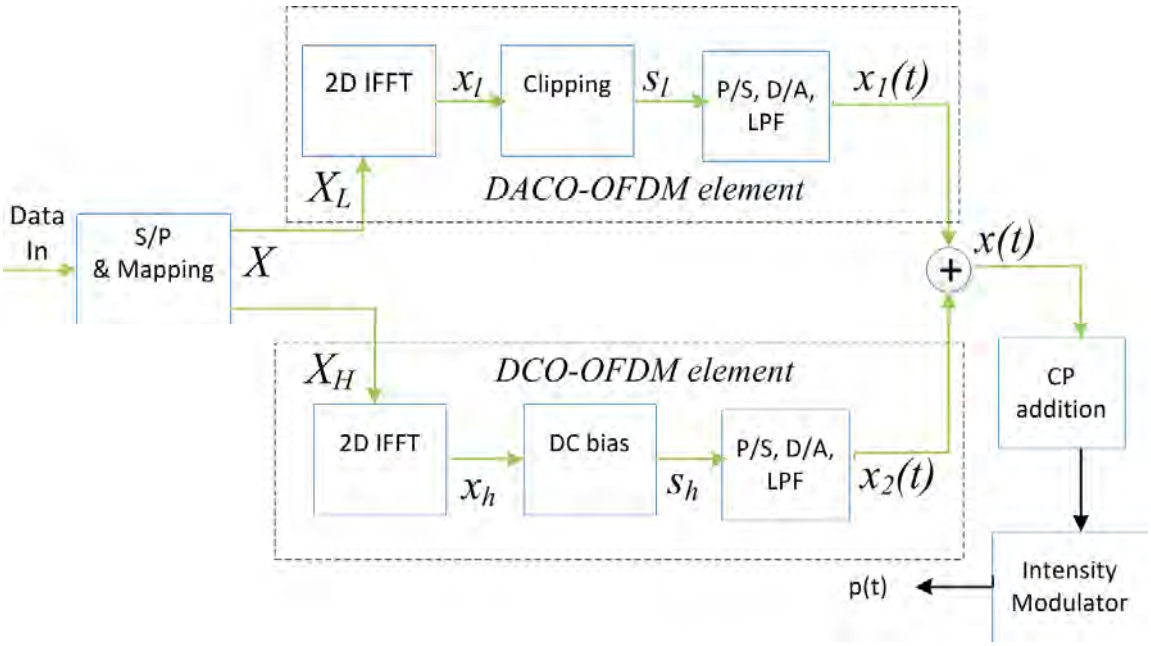

Figure 4-1: Block diagram of HDC-OFDM transmitter

In the transmitter, serial data are first converted to parallel and then mapped to the constellation points being used. For M-QAM based HDC-OFDM, the binary data will be mapped to the M constellation points. The resultant complex signal is given by

$$X = [X_0, X_1, X_2, X_3, ...X_{L-1,} X_{L,} .....X_{N-1}] \tag{2.45}$$

The X vector is constrained to have Hermitian symmetry and the two components X_0 and $X_{N/2}$ are set to zero which means $X_0 = X_{N/2} = 0$. It has already been mentioned that this symmetry is required to ensure that the output from the IFFT block is real. The Hermitian Symmetry condition can be defined as

$$X_m = X^*_{N-m} \text{ for } 0 < m < N/2 \tag{2.46}$$

Next, the complex signal X is divided into lower-index subcarriers, X_L, and higher-index subcarriers, X_H. The terms X_L and X_H are to be transformed into DACO-OFDM and DCO-OFDM, respectively. When only the independent data-carrying subcarriers are considered (excluding the Hermitian Symmetry portion), X_L can be represented as follows:

$$\begin{aligned} X_L &= [X_0, X_1, X_2, X_3, ...X_{L-1,} X_{L,} X_{L+1,} .....X_{N/2-1}] \\ &= [X_0, X_1, X_2, X_3, ...X_{L-1,} 0, 0.....,0] \end{aligned} \tag{2.47}$$

Similarly, X_H can be written as

$$\begin{aligned} X_H &= [X_0, X_1, X_2, X_3, ...X_{L-1,} X_{L,} X_{L+1,} .....X_{N/2-1}] \\ &= [0, \quad 0, \quad 0, \quad 0, ...0, \quad X_{L,} X_{L+1,} .....X_{N/2-1}] \end{aligned} \tag{2.48}$$

First, the case for X_L (the DACO-OFDM part) is considered**.** The complex signal X_L is input to an IFFT block resulting in a time domain real and bipolar signal x_l. The negative portion of the signal x_l is removed by clipping the amplitude at zero. The resultant unipolar signal s_l is then converted from parallel to serial (P/S) and Digital to

Analog (D/A). After these conversions, the signals are low pass filtered resulting in $x_1(t)$. This is the continuous time domain transmitted DACO-OFDM signal.

Now the case for X_H (the DCO-OFDM part) is considered. The complex signal X_H is input to an IFFT block resulting in a time domain real and bipolar signal x_h. The negative portion of the signal x_h is removed by adding a DC bias. The resultant unipolar signal x_h is then converted from parallel to serial (P/S) and Digital to Analog (D/A). After these conversions, the signals are low pass filtered resulting in $x_2(t)$. This is the continuous time domain transmitted DCO-OFDM signal.

Next, the DACO-OFDM and DCO-OFDM signals are added to form the HDC-OFDM transmitted signal $x(t)$:

$$x(t) = x_1(t) + x_2(t) \tag{2.49}$$

A cyclic prefix (CP) is added to $x(t)$ and then the resultant signal is input to an optical transmitter to generate optical signals $p(t)$. This is the HDCO-OFDM transmitted signal in the optical domain.

4.2.2 HDC-OFDM Receiver

The receiver of an HDC-OFDM system is shown in *Figure 4-2* **.**

The received optical signal $q(t)$ is added with additive white Gaussian noise (AWGN). Next, the signal is low pass filtered and converted to digital from analog. After that the CP is removed and the signal is converted into parallel streams. The parallel signal is passed through a single step frequency domain equalizer. The equalized signal, Y, is divided into lower-index subcarriers, Y_L, to perform DACO-OFDM demodulation, and higher-index subcarriers, Y_H, to perform DCO-OFDM demodulation.

First consider the demodulation of DACO-OFDM component. By excluding the Hermitian Symmetry part, the term Y_L can be expressed as

$$Y_L = [Y_0, Y_1, Y_2, Y_3, \ldots\ldots\ldots Y_{L-1,}\, 0, \ldots\ldots\ldots 0] \tag{2.50}$$

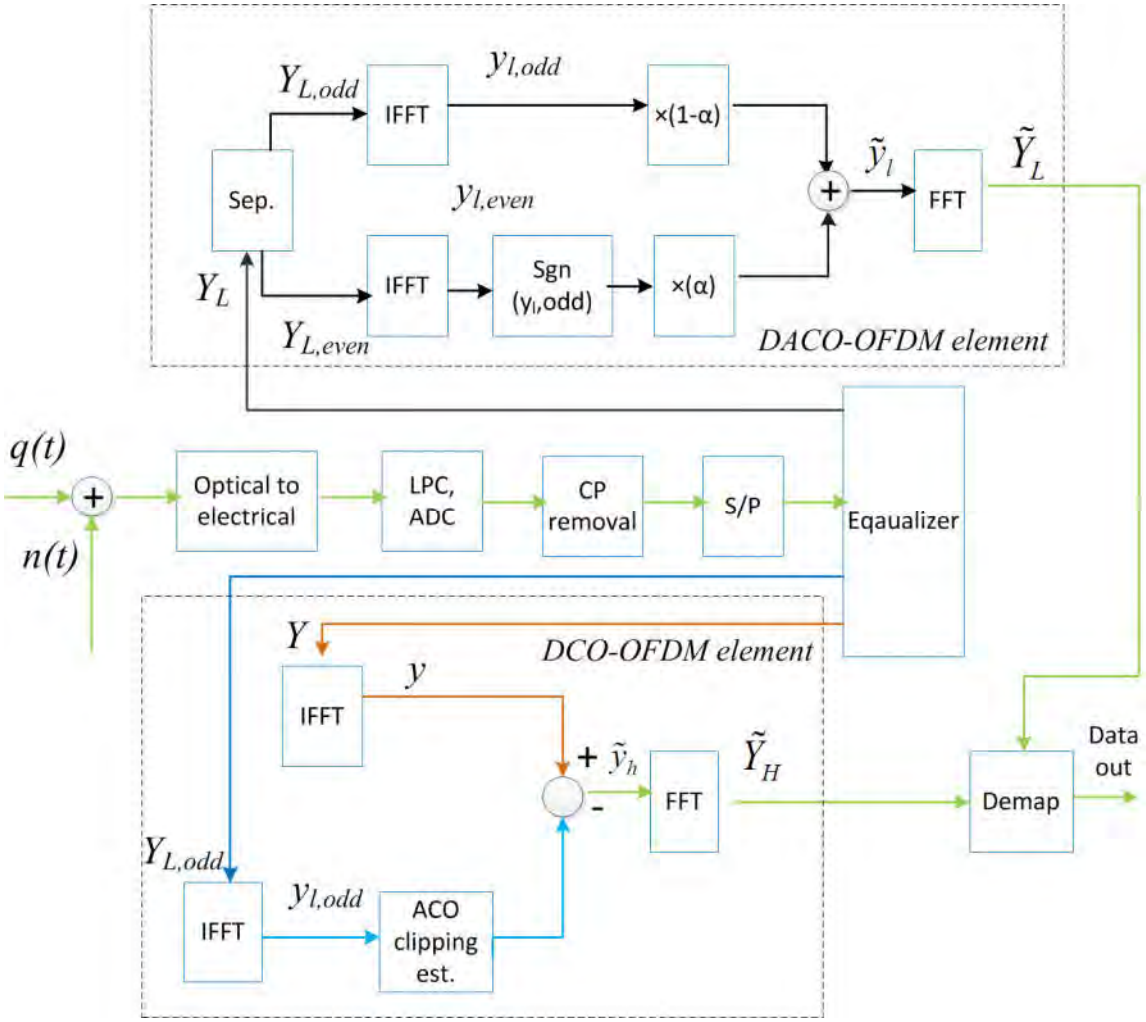

Figure 4-2: Block diagram of HDC-OFDM receiver

Next, Y_L is divided into odd-index subcarriers $Y_{L,odd}$ and even-index subcarriers $Y_{L,even}$. The term $Y_{L,odd}$ can be expressed as

$$Y_{L,odd} = [0, Y_1, 0_2, Y_3, 0 \ldots\ldots\ldots Y_{L-1,}\, 0, \ldots\ldots\ldots 0] \tag{2.51}$$

Similarly, $Y_{L,even}$ can be written as

$$Y_{L,even} = [Y_0, 0, Y_2, 0, Y_4 \ldots\ldots\ldots 0, 0, \ldots\ldots\ldots 0] \tag{2.52}$$

After that $Y_{L,odd}$ is converted to time domain signal $y_{l,odd}$ by taking an IFFT operation. On the other hand, $Y_{L,even}$ is converted to time domain signal $y_{l,even}$ by taking another IFFT operation. The terms $y_{l,odd}$ and $y_{l,even}$ are combined together to form an estimate of the time domain DACO-OFDM signal $\tilde{y}_l$ as follows:

$$\tilde{y}_l = (1-\alpha)\times y_{l,odd} + \alpha \times \operatorname{sgn}\left(y_{l,odd}\right) \times y_{l,even} \tag{2.53}$$

where α is a constant.

A FFT is computed on $\tilde{y}_l$ to form the frequency domain estimate of the DACO-OFDM signal, $\tilde{Y}_L$. The term $\tilde{Y}_L$ can be expressed as

$$\tilde{Y}_L = [\tilde{Y}_0, \tilde{Y}_1, \tilde{Y}_2, \tilde{Y}_3, ...\tilde{Y}_{L-1,}\, 0, ...0] \tag{2.54}$$

It can be noted that the clipping noise generated on DCO-OFDM signal impairs the performance of DACO-OFDM element. This is reduced by using a high DC bias on DCO-OFDM which results in less clipping noise.

Now, let us consider the DCO-OFDM demodulation. The combined signal, Y, obtained from the equalizer is converted to a time domain signal y by an IFFT operation. On the other hand, the $Y_{L,odd}$ signal obtained from the equalizer is converted to a time signal $y_{l,odd}$ by another IFFT operation.

It can be noted that when DACO-OFDM signal is generated in the transmitter side, a clipping noise is formed affecting the DCO-OFDM signal. At the receiver side, the DACO-OFDM clipping noise is estimated and then deducted from the received signal of DCO-OFDM. This clipping noise estimation technique is the one described in [22] for ADO-OFDM. This is explained in the following. The $y_{l,odd}$ signal is bipolar and thus is clipped at zero to estimate the DACO-OFDM clipping noise generated at the transmitter side. This resultant signal is deducted from the term y to form the time domain estimate

of DCO-OFDM signal $\tilde{y}_h$. The frequency domain equivalence of $\tilde{y}_h$ is generated by FFT operation forming $\tilde{Y}_H$. The term $\tilde{Y}_H$ can be expressed as

$$\tilde{Y}_H = [0,0,0,0,.....\tilde{Y}_{L,}\tilde{Y}_{L+1,}.....\tilde{Y}_{N/2-1}] \tag{2.55}$$

Next, $\tilde{Y}_L$ and $\tilde{Y}_H$ are added to form an estimated signal $\tilde{Y}$ as follows

$$\begin{aligned}\tilde{Y} &= \tilde{Y}_L + \tilde{Y}_H \\ &= [\tilde{Y}_0,\tilde{Y}_1,\tilde{Y}_2,\tilde{Y}_3,.....\tilde{Y}_{L-1,}\,0,.....0] + \\ &\quad [0,0,0,0,.....\tilde{Y}_{L,}\tilde{Y}_{L+1,}.....\tilde{Y}_{N/2-1}] \\ &= [\tilde{Y}_0,\tilde{Y}_1,\tilde{Y}_2,\tilde{Y}_3,.....\tilde{Y}_{L-1,}\tilde{Y}_{L,}\tilde{Y}_{L+1,}.....\tilde{Y}_{N/2-1}]\end{aligned} \tag{2.56}$$

The signal $\tilde{Y}$ is demapped to recover the original binary data.

4.3 Performance Evaluation of HDC-OFDM

In this section, investigations are carried out to evaluate the BER performance of HDC-OFDM based optical OWC. With the use of MATLAB tool, simulation results have been presented for an ideal AWGN optical channel with no other distortion. Simulations were carried out considering 256 subcarriers $(N = 256)$, a CP of 10 % and constellation sizes of M having values of 4 and 16. It can be noted that in ACO-OFDM, DACO-OFDM, only the odd subcarriers are modulated, whereas in DCO-OFDM, both the odd and even subcarriers are modulated for data transmission. Similarly for the case of HDC-OFDM for the DACO portion, only the odd subcarriers are modulated and the even subcarriers are kept unused; while for the DCO portion all the odd and even subcarriers are used to transmit data. In order to take this variation in the spectral efficiency of different modulation forms, the total transmitted optical power is normalized to unity.

The BER performance of HDC-OFDM is a function of the power level on DACO-OFDM and DCO-OFDM elements. *Figure 4-3* presents the plots for BER versus

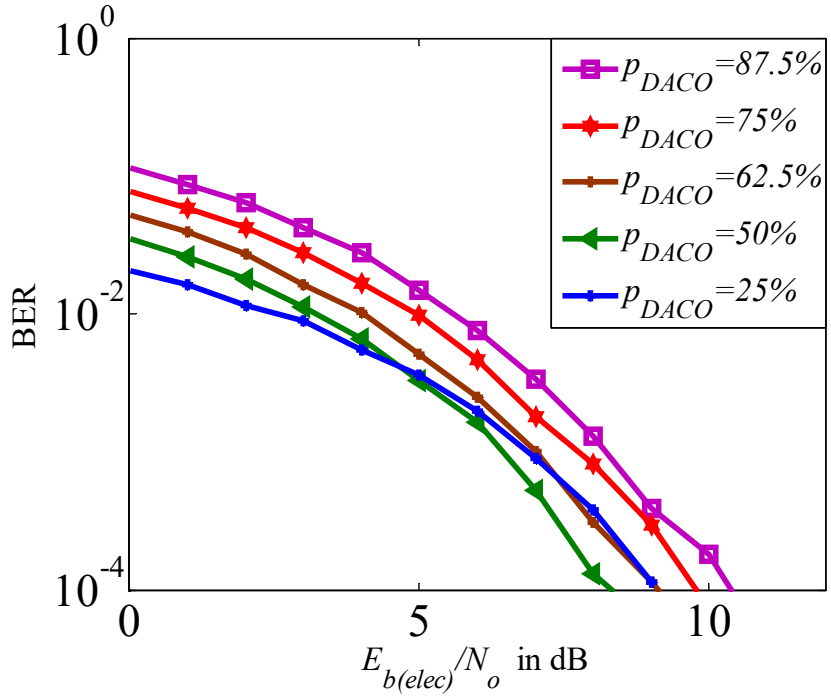

Figure 4-3: BER versus $E_{b(elect)}/N_0$ for 4-QAM HDC-OFDM for different power levels on DACO element

$E_{b(elect)}/N_0$ for 4-QAM HDC-OFDM for different percentage of power levels on DACO and DCO component. The percentage of subcarriers and power on DACO-OFDM is represented in the figure as p_{DACO} . For example, $p_{DACO} = 50\%$ means the power on DACO and DCO components is the same and the number of subcarriers belonging to DACO, $N/2$, is also the same as that of DCO-OFDM, $N/2$. It can be seen that the BER performance degrades when the values of p_{DACO} increase or decreases from the mid value. In other words, the best BER performance is achieved when p_{DACO} reaches 50%. The degradation is about 2 dB when the p_{DACO} value increases from 50% to 87.5%.

Next, the dimming flexibility of HDC-OFDM is evaluated. The dimming can easily be applied to HDC-OFDM by changing the bias of DCO-OFDM component. *Figure 4-4*

shows the plots of BER versus $E_{b(opt)}/N_0$ of 4-QAM HDC-OFDM for different dimming levels.

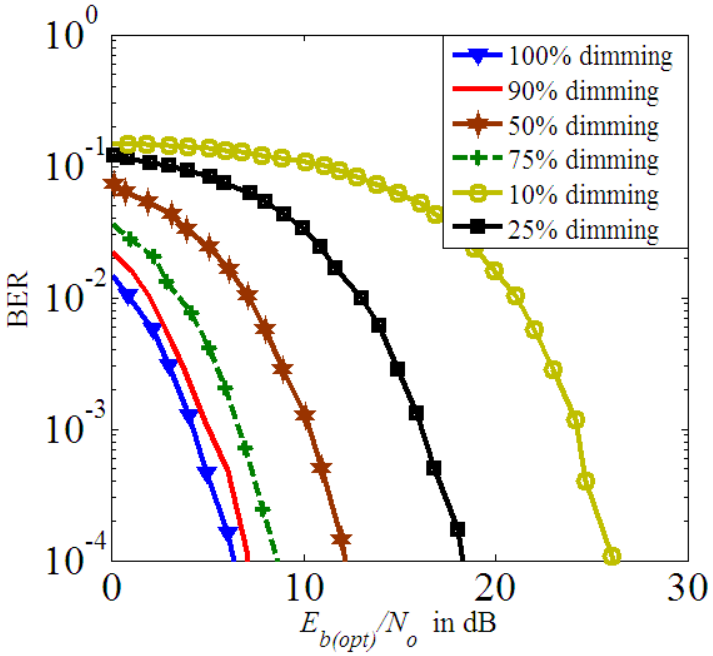

Figure 4-4: BER versus $E_{b(opt)}/N_0$ for 4-QAM HDC-OFDM for different dimming levels

In this thesis, a dimming level of 100% means full brightness, while 50% means half brightness or half optical power level. The transmitted optical power is varied according to the dimming level. It has already been mentioned that for simulations, the transmitted optical power is normalized to unity. This case (unity power) is assumed as 100% brightness. Therefore, for the case of 25% dimming the transmitted optical power becomes 0.25. It can be seen that when the brightness falls to 50% from 100%, there is almost 6 dB $E_{b(opt)}/N_0$ degradation. On the other hand, a dimming up to 10% is also possible however at the cost of 20 dB $E_{b(opt)}/N_0$ degradation.

4.4 Comparison of HDC-OFDM with other OFDM forms

In this section, the BER performance of HDC-OFDM is compared with DACO-OFDM and DCO-OFDM. Plots of ACO-OFDM and ADO-OFDM are also taken into comparison. Since only the odd subcarriers are used in ACO-OFDM, 16-QAM ACO-OFDM has to be compared with 4-QAM DCO-OFDM. The BER performance of ADO-OFDM depends on the levels of power on ACO-OFDM and DCO-OFDM elements within ADO-OFDM. It is shown in [22] that the optimum BER performance for 4-QAM ADO-OFDM is achieved when 70% of the optical power is loaded on ACO-OFDM component. So, when ADO-OFDM is considered in the simulations of this chapter, it is assumed that 70% power is on ACO-OFDM element and 30% power on DCO-OFDM component. The plots of BER versus $E_{b(elec)}/N_0$ are shown in *Figure 4-5*. The plots show that at a given BER of 10^{-4}, the BER performance of HDC-OFDM is 7 dB better than ADO-OFDM. Moreover, HDC-OFDM is 6 dB better than 4-QAM DCO-OFDM, 5 dB better than 16-QAM ACO-OFDM, but only 2 dB inferior to DACO-OFDM. Therefore, HDC-OFDM is very close to DACO-OFDM in terms of electrical power efficiency.

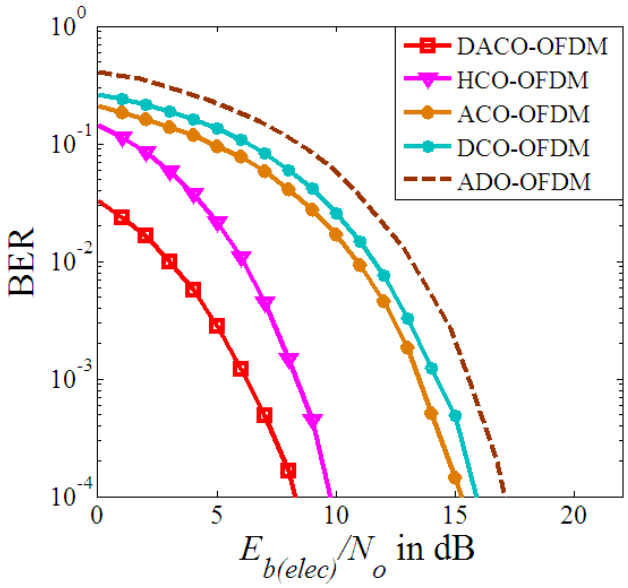

Figure 4-5: BER versus $E_{b(elec)}/N_0$ for 4-QAM HDC-OFDM, 4-QAM DCO-OFDM, 16-QAM ACO-OFDM, 4-QAM DACO-OFDM and 4-QAM ADO-OFDM

The plots of BER versus $E_{b(opt)}/N_0$ are shown in *Figure 4-6*. The plots show that for a given BER of 10^{-4}, the BER performance of HDC-OFDM is 8 dB better than 4-QAM DCO-OFDM and 4 dB better than 16-QAM ACO-OFDM; but only 1.5 dB inferior to DACO-OFDM. Furthermore, HDC-OFDM is almost 10 dB more optically power efficient than ADO-OFDM.

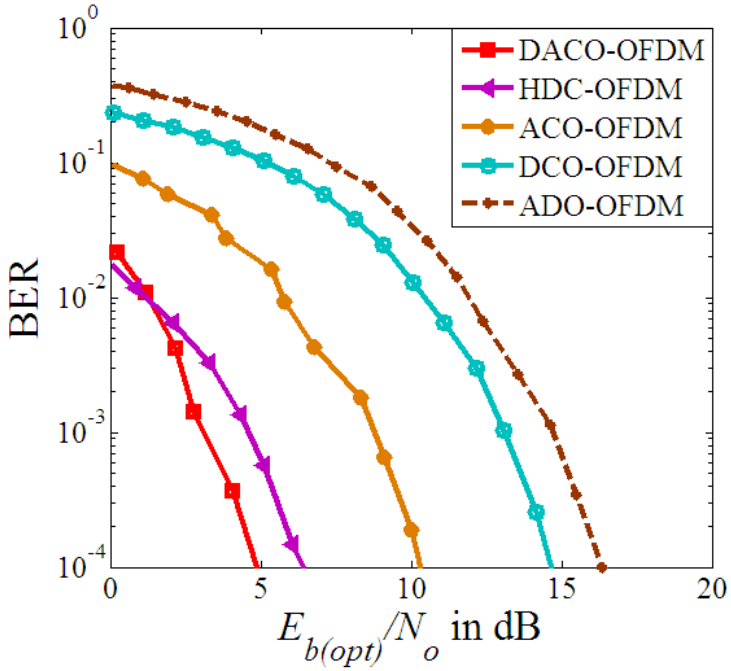

Figure 4-6: BER versus $E_{b(opt)}/N_0$ for 4-QAM HDC-OFDM, 4-QAM DCO-OFDM, 16-QAM ACO-OFDM and 4-QAM DACO-OFDM

Now, the modulation forms are compared considering the same overall data rate. It can be noted that like ACO-OFDM, DACO-OFDM uses only the odd subcarriers and thus provide half data rate. Therefore, 16-QAM stand-alone DACO-OFDM and 16-QAM ACO-OFDM have the same data rate as 4-QAM DCO-OFDM. Similarly, the DACO component within HDC-OFDM has only the odd subcarriers used for data transmission; however, the DCO-OFDM part has all the subcarriers useful. Therefore, to obtain the same data rate as 4-QAM stand-alone DCO-OFDM, the DACO component of HDC-OFDM should be mapped by 16-QAM and the DCO part by 4-QAM. *Figure 4-7*

presents different optical OFDM forms with the same overall data rate that is the same bits/sec/Hz. It can be seen that for a given data rate, HDC-OFDM (16QAM DACO & 4-QAM DCO) is only 1.5 dB less efficient than 16-QAM DACO-OFDM. However, this HDC-OFDM is now better than 16-QAM ACO-OFDM and 4-QAM DCO-OFDM by 1 dB and 5 dB, respectively. Moreover, HDC-OFDM is almost 7 dB more optically power efficient than ADO-OFDM.

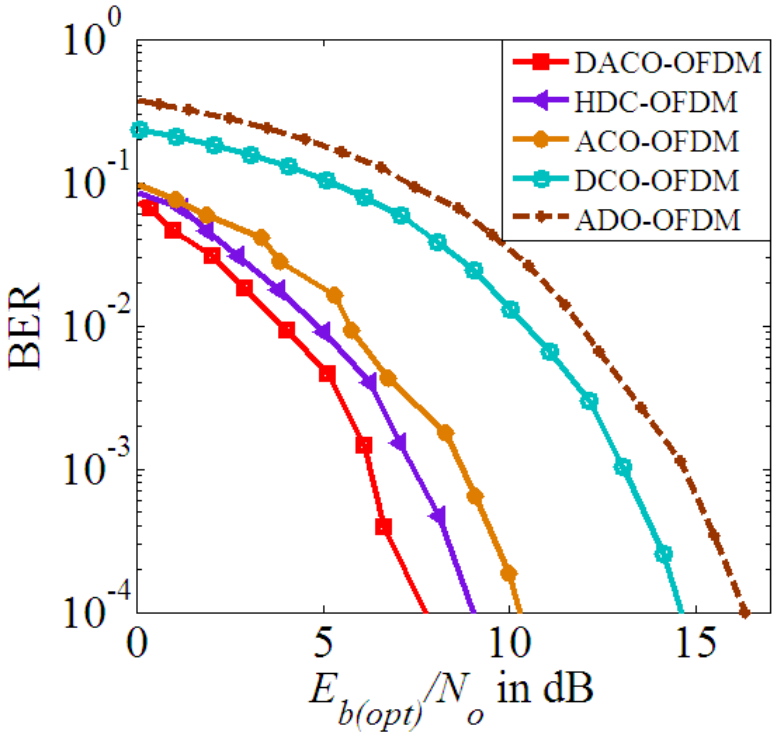

Figure 4-7: BER versus $E_{b(opt)}/N_0$ for HDC-OFDM (16QAM DACO & 4 QAM DCO), 4-QAM DCO-OFDM, 16-QAM ACO-OFDM and 16-QAM DACO-OFDM

4.5 Summary

The results presented in this chapter indicate that HDC-OFDM has almost retained the excellent power efficiency of DACO-OFDM and the dimming flexibility of DCO-OFDM. Therefore, HDC-OFDM is a promising modulation format for both data communication and room illumination.

5 CONCLUSION

5.1 Overview

OFDM based OWC systems have been presented in this thesis. Different forms of OFDM such as ACO-OFDM, DCO-OFDM, ADO-OFDM and DACO-OFDM have been described in different chapters.

The basic difference between ADO-OFDM and HDC-OFDM is that: in ADO-OFDM, odd frequency subcarriers are modulated by ACO-OFDM and even frequency subcarriers are modulated by DCO-OFDM whereas in our proposed HDC-OFDM, the lower frequency subcarriers are modulated by DACO-OFDM and higher frequency subcarriers are modulated by ACO-OFDM. Though the best performance can be achieved in case of 50% power and subcarrier proportions, there is no fixed rule that it has to be kept fixed on that value only, the power and subcarrier proportions can be varied according to the requirements of the system. On the other hand, in ADO-OFDM, the proportion of subcarriers is not changeable but the power proportion can be changed in this OFDM system.

The main contribution of this thesis is the development of HDC-OFDM as described in Chapter 4. This Chapter will provide concluding remarks on the thesis. The thesis contributions and the implications of the contributions are provided below:

5.2 Summary of the Findings of the Thesis

The findings of the thesis can be summarized as follows:

i) A framework for a new modulation format termed as ‘HDC-OFDM’ is proposed. HDC-OFDM combines the aspects of DCO-OFDM and DACO-OFDM. An important

point to note here is that HDC-OFDM is significantly different than the existing ADO-OFDM in two major ways. Firstly, ADO-OFDM merges ACO-OFDM and DCO-OFDM while HDC-OFDM combines DACO-OFDM and DCO-OFDM. Secondly, in ADO-OFDM only the odd subcarriers are modulated as ACO-OFDM and even as DCO-OFDM, while in HDC-OFDM all the lower subcarriers (including odd and even) are mapped to DACO-OFDM and all the higher subcarriers (including odd and even) are modulated as DCO-OFDM. The combining of DCO-OFDM and DACO-OFDM is not straightforward. The DACO-OFDM is computed on low-index subcarriers while DCO-OFDM on high-index subcarriers. When these two signals are added, they impact one another. The clipping noise generated on DCO-OFDM signal impairs the performance of DACO-OFDM element. This is reduced by using a high DC bias on DCO-OFDM which results in less clipping noise. On the other hand, when DACO-OFDM signal is generated in the transmitter side, a clipping noise is formed affecting the DCO-OFDM signal. At the receiver side, the DACO-OFDM clipping noise is estimated and then deducted from the received signal of DCO-OFDM.

ii) The performance results of HDC-OFDM are presented using MATLAB tool. The results indicate that the BER performance of HDC-OFDM varies depending on the proportion of DACO-OFDM and DCO-OFDM components. It is shown that the optimum performance is achieved when half the subcarriers are modulated by DCO-OFDM and the other half by DACO-OFDM – where the power levels on these two signals are set equal.

iii)Since the HDC-OFDM has a DCO-OFDM component, the dimming facility is easily achieved in HDC-OFDM by only increasing/decreasing the DC bias level without using any other additional modules or methods. Results show that when the dimming is 50%, there is a degradation of approximately 6 dB in terms of optical power. Simulation results also demonstrate that a dimming as low as 10% is also possible in HDC-OFDM at a 20 dB optical power degradation compared to full brightness conditions.

iv) Finally, it is shown that HDC-OFDM is almost as efficient as DACO-OFDM in terms of electrical and optical power. The difference in electrical or optical power

efficiency is within 2 dB. The performance of HDC-OFDM is at least 5 dB better than DCO-OFDM.

5.3 Implications of the Results of this Thesis

The simulation results on HDC-OFDM presented in this thesis are based on some specific parameters and conditions. For example only AWGN channels are considered which is often the case for short distance indoor OWC. Therefore, the results may vary when a dispersive channel (for instance, outdoor OWC) is taken into consideration. In HDC-OFDM, the lower subcarriers are modulated with DACO-OFDM and the higher subcarriers with DCO-OFDM. As long as a stand-alone AWGN channel is considered, the results will not change if the DACO-OFDM is mapped to higher subcarriers and DCO-OFDM at lower subcarriers. An important issue in this thesis is that the BER performance results are illustrated for a target BER of 10^{-4}. In a data communication scenario, a target BER of 10^{-9} is desirable. By the use of convolutional channel coding, the BER plots in this thesis can be extended to a BER of 10^{-9}.

Furthermore, when different optical OFDM forms are compared with HDC-OFDM, only 4-QAM and 16-QAM constellations are considered. The results may be different for constellations such as 256-QAM or 1024-QAM, etc. Only simulation results are presented for HDC-OFDM. These results may not be perfectly in agreement in a practical HDC-OFDM system where other factors are present such as channel effects, imperfect equalization, device error, etc.

5.4 Future Work

A perfect channel has been estimated in this thesis where only AWGN is present. Other kinds of noise, distortion and interference have been assumed to be zero. But a multipath dispersive channel can be considered in a future research in order to have an overall idea of the performance of the system in a real-life practical scenario. Channel coding is not included in the total calculation of the receiver BER performance, but it might be included in the future works for it can change the BER to a value around 10^{-9} which seems quite achievable in a real-life scenario.

For mapping the input data, only 4-QAM and 16-QAM have been used in our thesis whereas much higher constellations are being used for the purpose of communication now-a-days. It can be noted that higher order constellations provide higher data rate at the expense of power efficiency. Higher order constellation mapping and thorough analysis of the same can be a very timely addition in this case. Practical implementation of the HDC-OFDM is of utmost importance to see if the results perfectly match the theoretical results. In this thesis, the lower frequency subcarriers have been modulated with DACO-OFDM and higher frequency subcarriers have been modulated by DCO-OFDM. The process can be interchanged i.e. the lower frequency and higher frequency subcarriers can be applied DCO-OFDM and DACO-OFDM correspondingly in a multipath realistic channel and the changes can be tracked down for future research works.

Finally, the better BER performance which has been achieved at for equal number of power as well as subcarrier proportions at DCO-OFDM as well as DACO-OFDM calls for an analytical expression.

5.5 Summary

The proposed concept of HDC-OFDM shows promising BER and dimming performance when compared with existing modulation schemes of DACO-OFDM, ACO-OFDM, ADO-OFDM and DCO-OFDM. In future, HDC-OFDM will be compared with other OFDM forms that are being reported in very recent research papers. A practical implementation of HDC-OFDM is also required to validate the simulation results and check the feasibility of this new OFDM forms.

Nevertheless, more intense research on the theoretical and practical aspects of HDC-OFDM may reveal many interesting results.

References

[1] Li, T., Ni, Q., Malone, D., Leith, D., Xiao, Y., and Turletti, T., "Aggregation with fragment retransmission for very high-speed WLANs," IEEE/ACM Trans. Netw., vol. 17, pp. 591-604, Apr. 2009.

[2] Abichar, Z. and Chang, J. M., "Group-Based medium access control for IEEE 802.11n wireless LANs," IEEE Trans. Mobile Comput., vol. 12, pp. 304-317, Feb. 2013.

[3] Eldin, S. S., Nasr, M., Khamees, S., Sourour, E., and Elbanna, M., "LDPC coded MIMO OFDM-based IEEE 802.11n wireless LAN," in IFIP International Conference on Wireless and Optical Communication Networks (WOCN), Cairo, Egypt, Apr. 2009.

[4] Elgala, H., Mesleh, R., and Haas, H., "Indoor Broadcasting via White LEDs and OFDM," in *IEEE Transactions on Consumer Electronics*, vol. 55, no. 3, pp. 1127-1134, August 2009.

[5] O'Brien, D., Turnbull, R., Minh, H. L., Faulkner, G., Bouchet, O., Porcon, P., Tabach, M. E., Gueutier, E., Wolf, M., Grobe, L., and Li, J., "High-speed optical wireless demonstrators: conclusions and future directions," J. Lightw. Technol., vol. 30, pp. 2181-2187, 2012.

[6] Bandara, K. and Chung, Y.-H., "Novel colour-clustered multiuser visible light communication," Transactions on Emerging Telecommunications Technologies, vol. 25, pp. 579-590, 2014.

[7] Borah, D. K., Boucouvalas, A. C., Davis, C. C., Hranilovic, S., and Yiannopoulos, K., "A review of communication-oriented optical wireless systems," EURASIP Journal on Wireless Communications and Networking, vol. 2012, pp. 91, 2012.

[8] Elgala, H., Mesleh, R., and Haas, H., "Indoor optical wireless communication: potential and state-of-the-art," IEEE Commun. Mag., vol. 49, pp. 56-62, Sep. 2011.

[9] Kahn, J. and Barry J., "Wireless infrared communications," in Proc. IEEE, vol. 85, pp. 265-298, 1997.

[10] O'Brien, D., Katz, M., Wang, P., Kalliojarvi, K., Arnon, S., Matsumoto, M., Green, R., and Jivkova, S., "Short-range optical wireless communications," In Technologies for the Wireless Future: Wireless World Research Forum (WWRF), vol. 2, pp. 277-296, 2006.

[11] Green, R. J., Joshi, H., Higgins, M. D., and Leeson, M. S., "Recent developments in indoor optical wireless systems," IET Communications, vol. 2, pp. 3-10, 2008.

[12] Hranilovic, Steve. "Wireless Optical Communication Systems WIRELESS OPTICAL COMMUNICATION SYSTEMS." (2005).

[13] Wang, T. Q., Sekercioglu, Y. A., and Armstrong, J., "Hemispherical lens based imaging receiver for MIMO optical wireless communications," in IEEE Globecom OWC workshop, USA, Dec. 2012.

[14] Alwan, J., "Eye safety and wireless optical networks (WONs)," Electro-Optics Group, AirFiber Inc., Apr. 2001.

[15] Sandalidis, H. G., "Coded Free-Space Optical Links over Strong Turbulence and Misalignment Fading Channels," IEEE Trans. Commun., vol. 59, pp. 669-674, 2011.

[16] Jiang, L., Jin, S., Shimamoto, S., Fujikawa, C., and Kodate, K., "Experiment on space and time division multiple access scheme over free space optical communication," IEEE Trans. Consum. Electron., vol. 57, pp. 1571-1578, 2011.

[17] Chan, V. W. S., "Free-space optical communications," J. Lightw. Technol., vol. 24, pp. 4750-4762, 2006.

[18] Tsiftsis, T. A., Sandalidis, H. G., Karagiannidis, G. K., and Uysal, M., "Optical wireless links with spatial diversity over strong atmospheric turbulence channels," IEEE Trans. Wireless Commun., vol. 8, pp. 951-957, 2009.

[19] Jing, L. and Uysal, M., "Achievable information rate for outdoor free space optical communication with intensity modulation and direct detection," in IEEE Global Telecommunications Conference (GLOBECOM), 2003, pp. 2654-2658 vol.5.

[20] Langer, K. and Grubor, J., "Recent developments in optical wireless communications using infrared and visible light," in International Conference on Transparent Optical Networks (ICTON), Rome, Italy, Jul. 2007.

[21] Q. Wang et al., "FPGA-based layered/enhanced ACO-OFDM transmitter," 2017 Optical Fiber Communications Conference and Exhibition (OFC), Los Angeles, CA, 2017, pp. 1-3.

[22] Dissanayake, S. D. and Armstrong, J., "Comparison of ACO-OFDM, DCO-OFDM and ADO-OFDM in IM/DD Systems," J. Lightw. Technol., vol. 31, pp. 1063-1072, 2013.

[23] Kavehrad, M., "Sustainable energy-efficient wireless applications using light," IEEE Commun. Mag., vol. 48, pp. 66-73, 2010.

[24] Zeng, L., O'Brien, D., Minh, H., Faulkner, G., Lee, K., Jung, D., Oh, Y., and Won, E. T., "High data rate multiple input multiple output (MIMO) optical wireless communications using white LED lighting," IEEE J. Sel. Areas Commun., vol. 27, pp. 1654–1662, 2009.

[25] Hranilovic, S. and Kschischang, F. R., "A pixelated MIMO wireless optical communication system," IEEE J. Sel. Topics Quantum Electron., vol. 12, pp. 859–874, 2006.

[26] Agrawal, N. and Davis, C. C., "Design of free space optical omnidirectional transceivers for indoor applications using non-imaging optical devices," Proc. SPIE 7091, Free-Space Laser Communications VIII, 709107 (19 August 2008).

[27] Ramirez-Iniguez, R. and Green, R. J., "Optical antenna design for indoor optical wireless communication systems," International Journal of Communication Systems, vol. 18, pp. 229-245, 3 April, 2005.

[28] Ho, K. and Kahn, J. M., "Compound parabolic concentrators for narrowband wireless infrared receivers," Optical Engineering, vol. 34, pp. 1385-1395, Dec. 1994.

[29] Zeng, L., O'Brien, D. C., Minh, H., Faulkner, G., Lee, K., Jung, D., Oh, Y., and Won, E. T., "High data rate multiple input multiple output (MIMO) optical wireless communications using white LED lighting," IEEE J. Sel. Areas Commun., vol. 27, pp. 1654–1662, 2009.

[30] Azhar, A. H., Tran, T., and O'Brien, D. C., "Demonstration of high-speed data transmission using MIMO-OFDM visible light communications," in *2010 IEEE Globecom Workshops*, Miami, FL, 2010, pp. 1052-1056.

[31] Dambul, K. D., O'Brien, D. C., and Faulkner, G., "Indoor optical wireless MIMO system with an imaging receiver," *IEEE Photonics Technology Letters*, vol. 23, no. 2, pp. 97-99, Jan.15, 2011.

[32] Mesleh, R., Elgala, H., Hammouda, M., Stefan, I., and Haas, H., "Optical spatial modulation with transmitter-receiver alignments," in 2011 16th European Conference on Networks and Optical Communications (NOC), Newcastle-Upon-Tyne, 2011, pp. 1-4.

[33] Yun, G. and Kavehrad, M., "Spot diffusing and Fly-Eye receivers for indoor infrared wireless communications," in in Proceedings of the IEEE International Conference on Selected Topics in Wireless Communication, Vancouver, B.C., Canada, 1992, pp. 286-292.

[34] Djahani, P. and Kahn, J. M., "Analysis of infrared wireless links employing multibeam transmitters and imaging diversity receivers," IEEE Trans. on Commun., vol. 48, pp. 2077-2088, Dec. 2000.

[35] Alresheedi, M. T. and Elmirghani, J. M. H., "10 Gb/s Indoor Optical Wireless Systems Employing Beam Delay, Power, and Angle Adaptation Methods With Imaging Detection," J. Lightw. Technol., vol. 30, pp. 1843-1856, 2012.

[36] O'Brien, D., "Multi-input multi-output (MIMO) indoor optical wireless communications," in Conf. Record 2009 Asilomar Conf. Signals, Syst. Comput., Nov. 2009, Pacific Grove, CA, 2009, pp. 1636-1639.

[37] Wang, T. Q., Sekercioglu, Y. A., and Armstrong, J., "Analysis of an optical wireless receiver using a hemispherical lens with application in MIMO visible light communications," J. Lightw. Technol., vol. 31, pp. 1744-1754, Jun. 2013.

[38] Hranilovic, S. and Kschischang, F. R., "Short-range wireless optical communication using pixelated transmitters and imaging receivers," in IEEE Int. Conf. Commun, 2004, pp. 891–895, Vol.2.

[39] Wook, H. B. C., Komine, T., Haruyama, S., and Nakagawa, M., "Visible light communication with LED-based traffic lights using 2-dimensional image sensor," presented at the IEEE Consumer Communications and Networking Conference (CCNC), 8-10 Jan, *2006.*, 2006, pp. 243-247.

[40] Ashok, A., Gruteser, M., Mandayam, N. B., Silva, J., Varga, M., and Dana, K. J., "Challenge: mobile optical networks through visual MIMO," presented at the International Conference on Mobile Computing and Networking (Mobicom), Chicago, Illinois, USA, 20-24 Sep. 2010.

[41] Ashok, A., Jain, S., Gruteser, M., Mandayam, N., Yuan, W., and Dana, K., "Capacity of pervasive camera based communication under perspective distortions," presented at the IEEE International Conference on Pervasive Computing and Communications, Budapest, Hungary, Mar. 2014.

[42] Hao, T., Zhou, R., and Xing, G., "COBRA: color barcode streaming for smartphone systems," presented at the International Conference on Mobile Systems, Applications and Services (MobiSys), Lake District, UK, 25-29 Jun. 2012.

[43] Dimitrov, S. and Haas, H., "Information rate of OFDM-based optical wireless communication systems with nonlinear distortion," J. Lightw. Technol., vol. 31, no. 6, pp. 918-929, March15, 2013.

[44] Tabernero, A., Portilla, J., and Navarro, R., "Duality of log-polar image representations in the space and spatial-frequency domains," IEEE Trans. Signal Process., vol. 47, pp. 2469-2479, Sep. 1999.

[45] Premachandra, H. C. N., Yendo, T., Tehrani, M. P., Yamazato, T., Okada, H., Fujii, T., and Tanimoto, M., "LED Traffic Light Detection Using High-speed-camera Image Processing for Visible Light Communication," Information and Media Technologies, vol. 6, pp. 785-791, 2011.

[46] Armstrong, J., "OFDM for optical communications," J. Lightw. Technol., vol. 27, pp. 189-204, 2009.

[47] Ashok, A., Gruteser, M., Mandayam, N. B., Silva, J., Varga, M., and Dana, K. J., "Challenge: mobile optical networks through visual MIMO," in International Conference on Mobile Computing and Networking (Mobicom), Chicago, Illinois, USA, 20-24 Sep. 2010.

[48] Perli, S. D., Ahmed, N., and Katabi, D., "PixNet : LCD-Camera pairs as communication links," in Special Interest Group on Data Communication (SIGCOMM), New Delhi, India, Aug. 2010.

[49] Pei, C. C., Zhang, Z. C., Fang, W. X., and Zhang, S. J., "2D-DPSK for quasi-diffuse pixelated wireless optical," in IEEE International Conference on Communication Technology (ICCT), Jinan, China, 25-28 Sep. 2011.

[50] Perli, S. D., Ahmed, N., and Katabi, D., "PixNet: interference-free wireless links using LCD-camera pairs," presented at the International Conference on Mobile Computing and Networking (Mobicom), Chicago, Illinois, USA, Sep. 20-24 2010.

[51] Tahar, M., Wang, T. Q., Medina, M. F. G., Gonzalez, O., and Armstrong, J., "Experimental Demonstration of Diversity Combining for Asymmetrically Clipped Optical OFDM", IEEE Commun. Lett., vol. 20, no. 5, pp. 906-909, May 2016.

[52] Chen, L., Krongold, B., and Evans, J., "Diversity Combining for Asymmetrically Clipped Optical OFDM in IM/DD Channels", in Proc. Globecom, Honolulu, HI, USA, 2009, pp. 1-6.

[53] Grubor, J., Randel, S., Langer, K. D., and Walewski, J. W., "Broadband Information Broadcasting Using LED-Based Interior Lighting", IEEE/OSA J. Lightw. Technol., vol. 26, no. 24, pp. 3883-3892, Dec. 2008.

[54] Armstrong, J., and Schmidt, B. J. C., "Comparison of Asymmetrically Clipped Optical OFDM and DC-Biased Optical OFDM in AWGN", IEEE Commun. Lett., vol. 12, no. 5, pp. 343-345, May 2008.

[55] Armstrong, J., and Lowery, A. J., "Power Efficient Optical OFDM", Electron, Lett., vol. 42, no. 6, pp. 370-372, 2006.

[56] Wang, Y., Wang, Y., and Chi, N., "Experimental Verification of Performance Improvement for a Gigabit Wavelength Division Multiplexing Visible Light Communication System Utilizing Asymmetrically Clipped Optical Orthogonal Frequency Division Multiplexing", Photonics Res.., vol. 2, pp. 138-142, oct. 2014.

[57] Azhar, A. H., and O'Brien, D., "Experimental Comparisons of Optical OFDM Approaches in Visible Light Communications", in proc. IEEE Globecom Workshops, 2013, pp. 1076-1080.

[58] Dissanayake, S. D., and Armstrong, J., "Novel techniques for Combatting DC-Offset in Diversity Combined ACO-OFDM", IEEE Commun. Lett., vol. 15, no. 11, pp. 1237-1239, Nov. 2011.

[59] Vucie, J., et al., "513 Mbit/s Visible Light Communications Link Based on DMT-Modulation of a White LED", J. Lightw. Technol., vol. 28, no. 24, pp. 3512-3518, Dec. 2010.

[60] Dang, J., Zhang, Z. , and L. Wu, "Frequency-Domain DIversity Combining Receiver for ACO-OFDM System", in IEEE Photonics Journal, vol. 7, no. 6, pp. 1-10, Dec. 2015.

[61] Bao, X., Yu, G., Dai, J., and Zhu, X., "Li-Fi: Light Fidelity-a Survey", in Wireless Networks, vol. 21, issue 6, pp 1879-1889, Aug. 2015.

[62] Stefan, I. , Elgala, H., and Haas, H., "Study of dimming and LED nonlinearity for ACO-OFDM based VLC systems," *2012 IEEE Wireless Communications and Networking Conference (WCNC)*, Shanghai, 2012, pp. 990-994.

[63] Elgala, Hany; Little, Thomas D.C.; "Reverse polarity optical-OFDM (RPO-OFDM): dimming compatible OFDM for gigabit VLC links," in Optics Express, vol. 21, issue 20, p. 24288, October 2013.

[64] Yang, Y., Zeng, Z. , Cheng, J. and Guo, C., "Spatial dimming scheme for optical OFDM based visible light communication," Opt. Express 24, 30254-30263 (2016).